AWARD NUMBER: W81XWH-16-1-0085

TITLE: Using High-Precision Signaling Activity Imaging to Personalize Ras Pathway Inhibition Strategies in Neurofibromatosis

PRINCIPAL INVESTIGATOR: John Albeck

CONTRACTING ORGANIZATION: University of California, Davis
Davis, CA 95616

REPORT DATE: June 2019

TYPE OF REPORT: Annual

PREPARED FOR: U.S. Army Medical Research and Materiel Command
Fort Detrick, Maryland 21702-5012

# REPORT DOCUMENTATION PAGE

*Form Approved*
*OMB No. 0704-0188*



| 1. REPORT DATE | 2. REPORT TYPE | 3. DATES COVERED |
|---|---|---|
| June 2019 | Annual | 1 Jun 2018 - 31 May 2019 |

**4. TITLE AND SUBTITLE**
Using High-Precision Signaling Activity Imaging to Personalize Ras Pathway Inhibition Strategies in Neurofibromatosis

**5a. CONTRACT NUMBER**

**5b. GRANT NUMBER**
W81XWH-16-1-0085

**5c. PROGRAM ELEMENT NUMBER**

**6. AUTHOR(S)**
John Albeck, Taryn Gillies, Carolyn Teragawa, Heather Blizard, Michael Pargett

E-Mail: jgalbeck@ucdavis.edu

**5d. PROJECT NUMBER**

**5e. TASK NUMBER**

**5f. WORK UNIT NUMBER**

**7. PERFORMING ORGANIZATION NAME(S) AND ADDRESS(ES)**

UNIVERSITY OF CALIFORNIA, DAVIS
1850 RESEARCH PARK DR, STE 300
DAVIS CA 95618

**8. PERFORMING ORGANIZATION REPORT NUMBER**

**9. SPONSORING / MONITORING AGENCY NAME(S) AND ADDRESS(ES)**

U.S. Army Medical Research and Materiel Command
Fort Detrick, Maryland 21702-5012

**10. SPONSOR/MONITOR'S ACRONYM(S)**

**11. SPONSOR/MONITOR'S REPORT NUMBER(S)**

**12. DISTRIBUTION / AVAILABILITY STATEMENT**

Approved for Public Release; Distribution Unlimited

**13. SUPPLEMENTARY NOTES**

**14. ABSTRACT**

The goal of this project is to characterize differences in Ras pathway signaling, using live cell activity measurements in cell types and genetic contexts relevant to NF1. In our previous reports, we described the completed data collection for single-cell measurements of ERK activity in both cell lines and in patient-derived fibroblasts. In this reporting period, we performed additional experiments and quantitative analysis to confirm our findings and to collate our data into a unified model of signal transmission by the Ras/ERK cascade. This model explains the finding that NF1-deficient cells, similar to Ras mutant cells, have an increased baseline of ERK activity in the absence of growth factors, but no increase in ERK amplitude upon growth factor stimulation. We show that the mechanism for this effect is distributed and includes regulation of phosphatase activity and a cryptic saturation point at Ras-Raf . Altogether, our results answer the central question of our project by demonstrating that the primary signaling defect in NF1-deficient cells is one of increased tonic ERK signaling, not of increased intensity.

**15. SUBJECT TERMS**

| 16. SECURITY CLASSIFICATION OF: | | | 17. LIMITATION OF ABSTRACT | 18. NUMBER OF PAGES | 19a. NAME OF RESPONSIBLE PERSON |
|---|---|---|---|---|---|
| a. REPORT | b. ABSTRACT | c. THIS PAGE | | | USAMRMC |
| Unclassified | Unclassified | Unclassified | Unclassified | 14 | 19b. TELEPHONE NUMBER *(include area code)* |

**TABLE OF CONTENTS**

**INTRODUCTION:** Many of the pathological effects of *NF1* mutations result from failure to regulate the activity of the Ras signaling pathway. Inhibition of this pathway is one of the major therapeutic strategies currently being explored for NF1 patients. The effectors of the Ras pathway include the Raf/MEK/ERK signaling cascade, which stimulates proliferation and controls the expression of many downstream genes. Recent cell biology studies have shown that the kinetics of ERK activation, including the intensity, duration, and probability of response, are critical for deciding how the cell responds to Ras activation and which genes are expressed. We have also found that different inhibitors of the Ras pathway have unique effects on these kinetic features and on cellular proliferation and gene expression. Therefore, an understanding of kinetic changes in kinase activity and their effects at the cellular level is important in designing effective inhibition strategies. Our preliminary studies demonstrate our ability to resolve these kinetic differences at high temporal resolution using high-throughput live-cell imaging of ERK, while similar measurements are not possible using traditional biochemical methods. The goal of this project is to develop reporter cells and perform real-time signaling activity measurements in cell lines and genetic configurations relevant to NF1, to determine whether *NF1* mutant cells differ in signaling intensity, duration, threshold, or basal activity. We also investigate how ERK kinetics in wild type and *NF1* mutant cells respond to a panel of pathway inhibitors to determine which dose levels and inhibitors represent the best strategy for normalizing mutant signaling activity and cell responses.

**KEYWORDS:** *Provide a brief list of keywords (limit to 20 words).* Ras, ERK, Akt, live-cell imaging, FRET reporter, inhibitor, kinetics.

**ACCOMPLISHMENTS:** *The PI is reminded that the recipient organization is required to obtain prior written approval from the awarding agency Grants Officer whenever there are significant changes in the project or its direction.*

**What were the major goals of the project?**

The main goal of this research project is to characterize the kinetic differences in Ras-driven signaling between wild type and NF1-deficient cells. The tasks and objectives are as follows:

| **Specific Aim 1 - Identify the kinetic differences in Ras effector activity resulting from NF1 mutations** | **Timeline** | **Site 1** |
|---|---|---|
| **Major Task 1 *Establish and validate isogenic reporter cell line models carrying NF1 mutants*** | Months | |
| Obtain CRISPR reagents, generate NF1+/- and -/- astrocyte, Schwann cells, and C2C12s | 1-3 | 100% |
| Transfect/transduce C2C12 and MPNST cell lines, select, and test by live-cell microscopy. | 4-6 | 100% |
| Transfect immortalized astrocyte and Schwann cells, test by live-cell microscopy. | 6-9 | 100% |
| Milestone(s) Achieved | | |
| Stable reporter cell lines for initial test, NF1 | 3 | 100% |
| Optimized imaging protocol and analysis pipeline | 6 | 100% |

| | | |
|---|---|---|
| All stable reporter cell lines ready | 9 | 100% |
| **Major Task 2** ***Measure and compare kinetic modes of ERK and Akt activity in NF1 wild type and mutant cell lines*** | Months | Completion |
| Collect data for different growth factor stimulation conditions | 6-12 | 100% |
| Extract data and perform quality control on dataset. | 6-14 | 100% |
| Perform statistical comparisons | 12-16 | 100% |
| Milestone(s) Achieved: | 4 | |
| Full dataset collected | 15 | 100% |
| Grid of statistical comparisons complete | 16 | 100% |
| | | |
| **Major Task 3** ***Measure ERK and Akt kinetics in patient-derived cells*** | Months | Completion |
| Develop stable reporter cells and optimize imaging protocol | 12-15 | 100% |
| Collect full dataset, extract data, perform quality control | 14-18 | 100% |
| Perform statistical comparisons | 16-18 | 80% |
| Milestone(s) Achieved: | | |
| Dataset collected | 18 | 100% |
| Statistical data available | 19 | 80% |
| | | |
| **Major Task 4** ***Correlate signaling kinetics with cellular behaviors*** | | |
| Perform live-cell and immunofluorescence experiments | 16-20 | 80% |
| Data analysis | 20-24 | 50% |
| Milestone(s) Achieved: | | |
| Data set collected | 20 | 80% |
| Table of similarity measurements completed | 24 | 20% |

| **Specific Aim 2 - Identify the Ras pathway inhibitors that best normalize signaling kinetics, gene expression, and cell proliferation rates for NF1 mutant cells.** | **Timeline** | **Site 1** |
|---|---|---|

| **Major Task 1** ***Identify Ras-pathway inhibitors that reverse single-cell NF1 kinetic modes and responses in cell lines*** | Months | Completion |
|---|---|---|
| Perform live-cell inhibitor experiments | 20-24 | 100% |
| Image data extraction and data set assembly | 20-26 | 90% |
| Statistical analysis and comparisons | 26-30 | 20% |
| Milestone(s) Achieved | | |
| Dataset collected | 24 | 100% |
| Statistical data available | 30 | 20% |
| **Major Task 2** ***Compare drug responses between different patient-derived cells*** | | |
| Collect inhibitor data on patient cell lines | 18-24 | 100% |
| Image data extraction and data set assembly | 22-25 | 100% |
| Statistical analysis and comparisons | 28-32 | 40% |
| Milestone(s) Achieved: | | |
| Dataset collected | 26 | 100% |
| Statistical data available | 32 | 20% |
| **Major Task 3** ***Link gene expression in response to Ras pathway inhibitors to cellular responses*** | | |
| Perform inhibitor treatment and proliferation/differentiation assays | 24-30 | 20% |
| Collect mRNA samples and perform mRNAseq. | 24-30 | 0% |
| Data analysis | 28-32 | 0% |
| Milestone(s) Achieved | | |
| Cell behavior data available | 30 | 0% |
| mRNAseq data available | 30 | 0% |
| Comparison of inhibitor data complete | 32 | 0% |
| **Major Task 4** ***Characterize individual cell adaptive responses to Ras pathway inhibitors in MPNST cells*** | | |
| Perform live-cell imaging of inhibitor treatment in MPNST cells | 30-32 | 0% |
| Extract image data and perform analysis | 32-36 | 0% |
| Milestone(s) completed | | |
| Image data set available | 34 | 0% |

| | | |
|---|---|---|
| Statistical comparisons complete | 36 | 0% |

**What was accomplished under these goals?**

Our work during this period was focused on validating and organizing our previous results into a unified model for Ras/ERK signal transduction properties. This work required a large number of quantitative immunoblot validation experiments and careful statistical analysis of these data alongside our live-cell experiments. We have completed a manuscript detailing this analysis and the resulting model, which is attached as an appendix to this report. This manuscript describes the general dynamic behavior of Ras mutants, which is highly similar to that of *NF1* mutants (see previous annual report); while *NF1* cells are included in this dataset, by agreement with our collaborators, the specific *NF1* mutant cell data will be described in a separate manuscript currently in preparation.

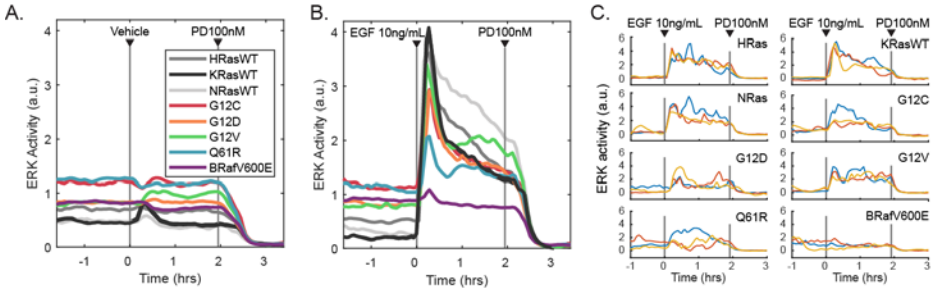


**Figure 1.** ERK activation by Ras mutants is limited to unstimulated conditions. MEFs expressing only the indicated forms of Ras were cultured in the absence of growth factors (A), or stimulated with EGF (B). Population means are shown in A and B. Example single cell recordings are shown in C.

In the single-cell data shown in our previous report, the most striking observation is that Ras-mutant and *NF1*-deficient cell lines show an increased baseline of ERK activity, but no increase in the peak ERK activity upon stimulation (Fig. 1). A careful review of the literature with respect to this observation reveals a high degree of ambiguity: the mutational status of Ras is poorly correlated with average phospho-ERK levels in both tumor cell lines (Omerovic et al., 2008; Yeh et al., 2009) and in genetically engineered mouse models (Tuveson et al., 2004). Counter-intuitively, conversion of a wild type Ras gene to a mutant can *reduce* average ERK activation (Tuveson et al., 2004). Ectopic expression of Ras mutants, however, can drive strong over-activation of ERK (Konishi et al., 2007; Park et al., 2006), as expected. Therefore, we viewed the dataset we collected on isogenic MEF cells carrying either wild type or mutant Ras as an important opportunity to clarify how mutational status alters ERK output, and to investigate the underlying mechanism. We believe this work will have a significant impact on the Ras signaling field by

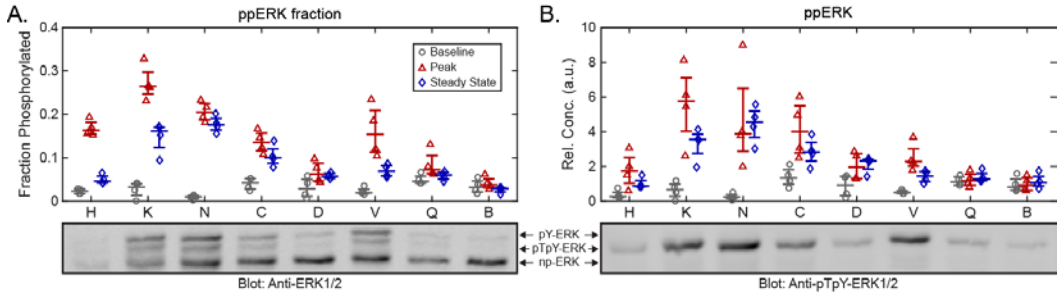


**Figure 2.** Immunoblotting to compare ERK activation peak intensity. MEFs engineered to express a single Ras isoform (H=$HRas_{WT}$, K=$KRas_{WT}$, N=$NRas_{WT}$, C=$KRas_{G12C}$, D=$KRas_{G12D}$, V=$KRas_{G12V}$, Q=$KRas_{Q61R}$, B=$BRaf_{V600E}$) were left unstimulated, or stimulated with EGF for short (peak) or long (steady state) times. A shows a Phos-tag immunoblot, in which phosphorylated and unphosphorylated ERK are resolved. B shows an immunoblot with a phospho-specific ERK antibody.

reconciling the apparently conflicting effects that have been reported.

A rudimentary potential mechanism for the limited peak ERK value could be saturation of either the reporter or the pathway itself. To investigate this possibility, we performed multiple immunoblot analyses. The most informative was a phos-tag analysis that we performed to separate the phosphorylated and unphosphorylated forms of ERK (Fig. 2). This analysis demonstrated that maximal stimulation by EGF only induced phosphorylation of approximately 30% of ERK, indicating that the pathway is not saturated at this level. Similarly, phos-tag analysis of the reporter showed that the pathway's activity remained well within its dynamic range across all conditions (Fig. 3). Thus, simple saturation, at least of the terminal kinase of the pathway and its substrates, cannot explain the peak limitation.

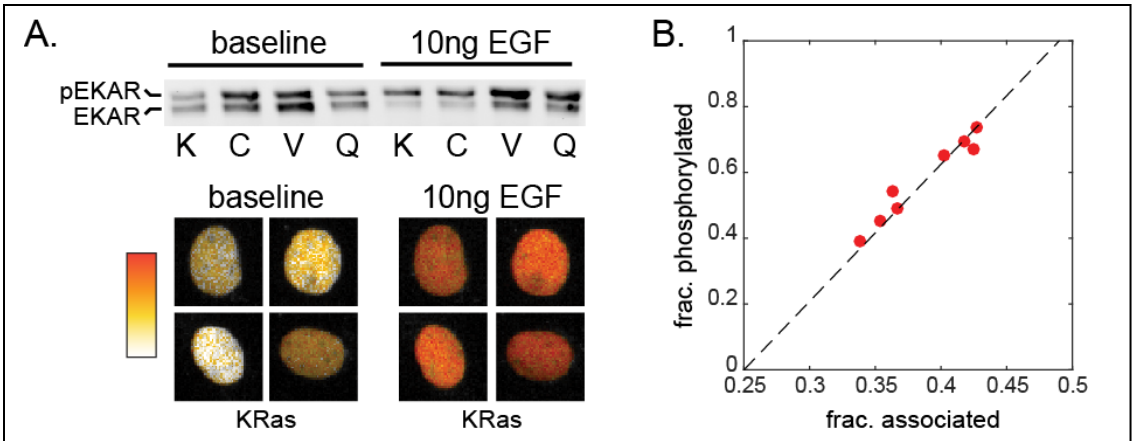


**Figure 3.** Assessment of reporter dynamic range. A. Phos-tag blot of the EKAR FRET reporter under unstimulated or stimulated conditions. Sample FRET ratio images of EKAR3-expressing nuclei are shown below. B. Comparison of FRET signal (frac. associated) to the fraction phosphorylated as determined by immunoblot reveals a linear relationship that is not saturated. Letter codes for Ras isoforms are as in Figure 2.

We then examined whether differences at the single cell-level could explain the limitation on ERK. Analysis of individual cell data revealed a potential bias in the average: the percentage of cells with a detectable ERK response was greatly reduced in mutant lines (Fig. 4). To determine if reduced response detection could simply be attributed to smaller amplitudes as the baseline activity increases, we assessed correlation with baseline activity. While the response rate does vary with average baseline activity (Fig. 4B), correlation at the single cell level is quite poor; many high baseline cells clearly respond and many low baseline cells do not, regardless of cell line (Fig. 4C). Thus, the population-averaged peak ERK activity is reduced in mutant cells by a lowered response probability unrelated to current ERK activity. However, even when we filtered the ERK activity dataset and used only traces with a distinguishable response, the peak responses in responding mutant cells were equivalent or lower in magnitude than wild type. Thus, stochastic responsiveness does not explain the peak limitation. Rather, the common upper bound on ERK activity suggests the existence of mechanisms that tightly regulate the peak.

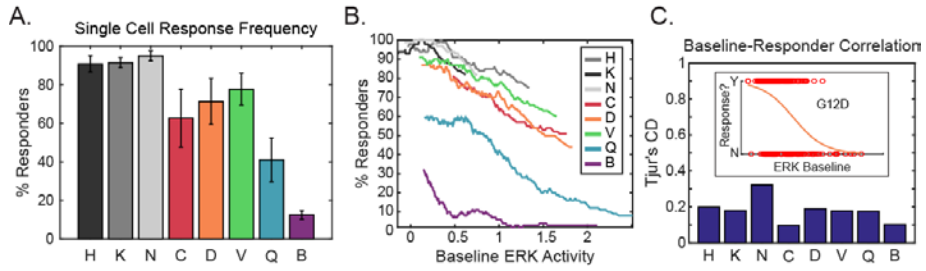


**Figure 4.** Reduced Fraction of ERK responses in Ras mutant cells. A. Bars indicate the fraction of cells showing an above-baseline response detected by EKAR3 following EGF stimulation. B. Lineplots show the % of responding cells as a function of the baseline ERK activity for each cell. C. Low correlation between baseline ERK activity level and likelihood of response for different Ras isoforms.

Even though the cell lines used were isogenic, expression levels of the pathway can vary across cell lines, due to epigenetic differences. We evaluated these differences by immunoblot. Compared with the wild type K-Ras cells, Ras levels were higher in G12C and G12V lines, lower in H-Ras, and as expected, negligible

in BRafV600E (Fig. 5). Levels of BRaf, MEK and ERK, but not CRaf, varied significantly among cell lines, without an obvious pattern or correlation structure. To quantitatively assess how the phospho-ERK measurements differ from simple expectations of Ras-driven activity, we constructed a "naïve" mathematical model (Fig. 6), which incorporates pathway expression levels (this study) as well as biochemical activity of Ras mutants (Gremer et al., 2011; Hunter et al., 2015; Smith et al., 2013), but does not model feedback regulation. The purpose of this model is to predict the ERK output that would be expected from the known differences in Ras isoforms (i.e. rate of GTP exchange and hydrolysis, affinity for Raf). Using a steady state solution of the naïve model, we predicted the baseline and steady state levels of phospho-ERK for each mutant cell line (Fig. 6A, B). Experimentally measured phospho-ERK was much lower in Ras mutants than predicted, especially at baseline. Conversely, the amplitude (fold change) in ERK with stimulation is greater in the real system than the naïve model, except for Q61R where differences are indistinguishable. Based on this comparison, the feedback regulation not included in the model effectively suppresses ppERK, but also potentially amplifies the response to growth factor stimulation.

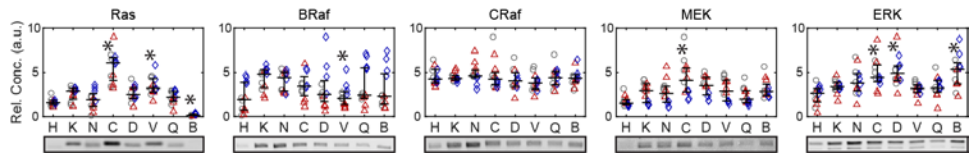


**Figure 5.** Immunoblot analysis of protein levels in Ras single isoform-expressing MEFs. Blots are shown at bottom, with quantification of multiple blots shown above. Lettering for isoforms is as in Fig. 2.

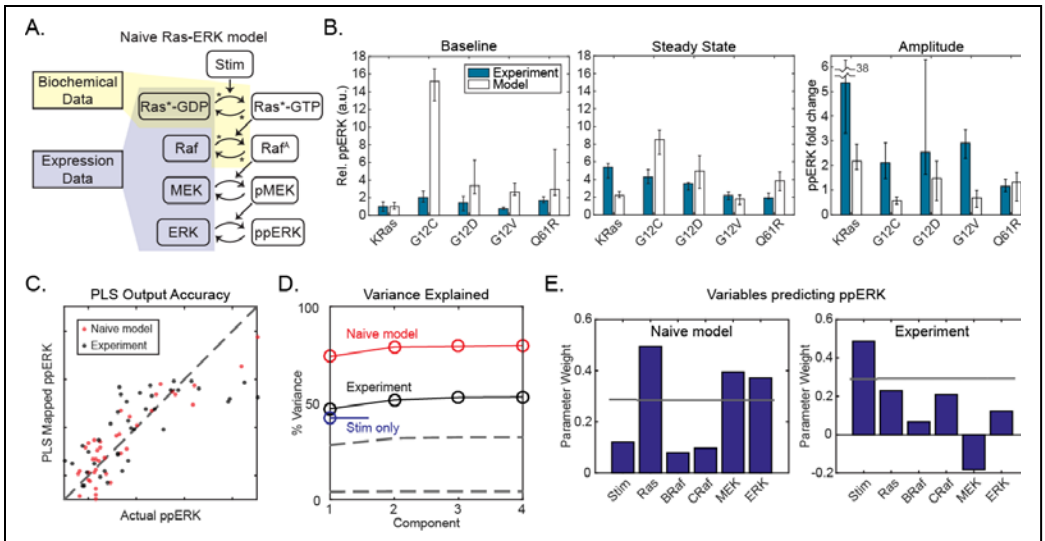


**Figure 6.** Modeling ERK output as a function of pathway expression levels and Ras biochemical properties. A. Schematic of model. B. Comparison of predicted vs. measured ERK output. At baseline and steady state, model values are typically higher than what is measured, while measured ERK activity is higher during at the peak amplitude following ERK stimulation. C. Partial least squares comparison of model and experimental ERK output. D. Experimental variance explained by the PLS model. E. Weights of pathway expression levels in predicting phospho-ERK output.

To determine how individual expression levels contribute to phospho-ERK levels, we employed partial least square regression (PLSR), fitting phospho-ERK against the levels of each pathway member and the presence of stimulation. The PLSR was repeated for the naïve model predictions of phospho-ERK to compare dependencies with and without feedback regulation. Both experimental and naive model phospho-ERK are correlated to expression and stimulation (Fig. 6C), and as expected less of the experimental variance is explained than for the naïve model (Fig. 6D). While modeled phospho-ERK was predominantly correlated with expression of Ras, MEK and ERK, experimental phospho-ERK was significantly correlated only with the presence of stimulation (Fig. 6E). We can therefore conclude that the unmodeled regulation in the pathway also provides robustness to expression level variation.

It is striking that stimulated ERK activity was nearly consistent across cell lines, but phospho-ERK level varied; this difference implicates variation in phosphatase activity, as the only variable theoretically separating our measurements of ERK phosphorylation and activity. Comparing the ERK activity and phospho-ERK averages for each cell line and time point, a significant linear relationship is evidenced among cell lines at

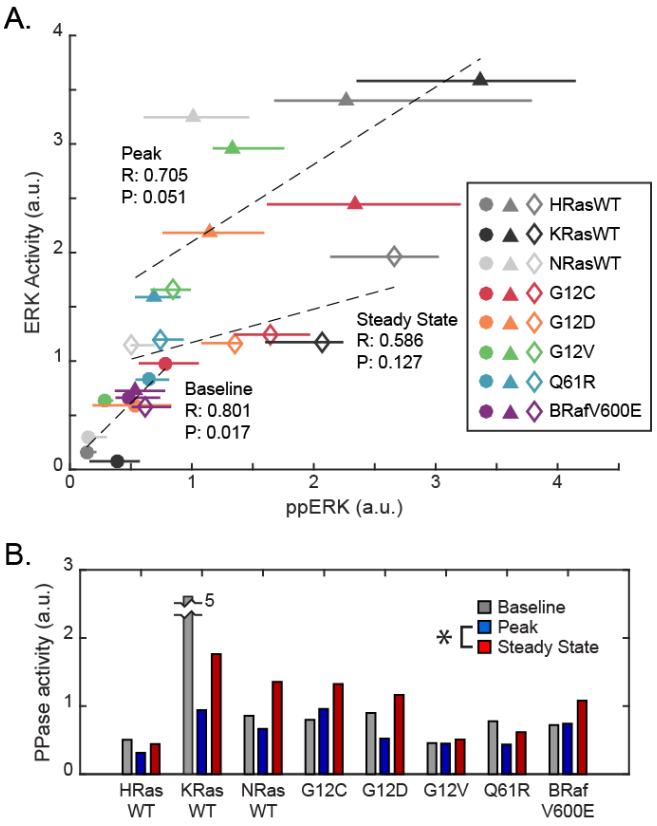


**Figure 7.** ERK activity (measured by FRET) as a function of ERK phosphorylation (measured by immunoblot). A. Linear fits are shown for samples collected under unstimulated (baseline, circles), peak stimulation (10 ng/ml EGF, 15 min, triangles), and steady state (10 ng/ml EGF >2 hours, diamonds). B. Estimation of phosphatase activity from the data in A, showing a drop in apparent phosphatase activity during peak EGF stimulation, followed by a rebound.

baseline, implying near constant phosphatase activities (Fig. 7A). However, while stimulation increases both phospho-ERK and ERK activity, their correlation across cell lines is progressively diminished at the peak and steady state time points. This change implies that phosphatase activity may be coordinated to maintain a target level of stimulated ERK activity.

To clarify the impact of phosphatases, we estimated the substrate phosphatase activity as the ratio of ppERK to ERK activity averaged over all replicates for each cell line and time point (Fig. 7B). Phosphatase activity is nearly uniform at baseline, with KRas as a notable outlier without explanation; the effect could reflect an isoform-specific function, or merely the nature of the single cloned K-Ras cell line. This behavior implies some involvement of feedforward control from growth factor stimulation, as phosphatase activity is not always correlated to ppERK, only after stimulation. The phosphatase response further evidences a coherent dynamic pattern following stimulation, with a significant rise in activity between peak and steady state times ($p = 0.005$), accounting for 40% - 70% of the drop in ERK activity after 1 hour of stimulation. These analyses support a model where phosphatase activity sharpens the growth factor response and normalizes stimulated ERK activity levels, potentially being immediately inhibited but stimulated after a delay, thus suppressing steady state ERK activity.

While it has been suggested that suppression of ERK in mutant Ras cells results mainly from negative feedback from ERK (Courtois-Cox et al., 2006), our systematic analysis reveals a more complex situation with multiple contributing factors. ERK-mediated negative feedback does play a role in restraining MEK activation, but we also find that Ras-mutant cells have a reduced probability of response that is independent of their current ERK activity and contributes to a lower pERK signal on immunoblots (in which all cells are averaged). Yet, even when this effect is accounted for in single cells, ERK responses remain limited in amplitude in Ras-mutant cells. In addition, phosphatase regulation decreases systematically in K-Ras mutants relative to wild type K-Ras. Thus, multiple mechanisms act together to rescale ERK activity when the pathway is activated by mutations at the level of Ras or NF1.

**What opportunities for training and professional development has the project provided?**

Nothing to report.

**How were the results disseminated to communities of interest?**

In addition to publications, results from this project were presented in oral presentations at the following meetings:

- qBio Summer School, Houston, TX, June 2018
- Max Planck Institute (IMPRS-CMB) International Student Symposium, November 2018
- International Meeting on Optical Biosensors, Ghent, Belgium, November 2018

**What do you plan to do during the next reporting period to accomplish the goals?**

Our work to date demonstrates that ERK signaling in Ras-mutant or NF1-deficient cells is different from wild type cells primarily in the baseline activity of ERK type cells. These findings raise the question of how these relatively small changes result in changes in cell behavior that ultimately have a large impact on tissue physiology. One possibility consistent with our data (Gillies et al., 2017), is that small changes in signaling activity over time lead to a large cumulative change at the level of gene expression. We will therefore place particular emphasis on Aim 2, Task 3, in which gene expression profiles will be linked to changes in signaling activity. We plan to carry out this aim using new technologies now available to our lab, including single-cell mRNA sequencing by drop-Seq.

**IMPACT:** *Describe distinctive contributions, major accomplishments, innovations, successes, or any change in practice or behavior that has come about as a result of the project relative to:*

**What was the impact on the development of the principal discipline(s) of the project?**

Within cancer biology, work from this project has led to an increasing recognition of the importance of signaling dynamics in controlling gene expression. An example citation of our work in this context:

Köhler M, Ehrenfeld S, Halbach S, Lauinger M, Burk U, Reischmann N, Cheng S, Spohr C, Uhl FM, Köhler N, Ringwald K, Braun S, Peters C, Zeiser R, Reinheckel T, Brummer T. (2019) B-Raf deficiency impairs tumor initiation and progression in a murine breast cancer model. *Oncogene* 38(8):1324-1339. doi: 10.1038/s41388-018-0663-8.

**What was the impact on other disciplines?**

The methods for ERK activity recording that we have developed are used increasingly in developmental biology. Examples of citations of our work in this context:

Deathridge J, Antolović V, Parsons M, Chubb JR. (2019) Live imaging of ERK signalling dynamics in differentiating mouse embryonic stem cells. *Development* 146(12). pii: dev172940. doi: 10.1242/dev.172940.

Johnson HE, Toettcher JE (2019) Signaling Dynamics Control Cell Fate in the Early Drosophila Embryo. *Dev Cell* 48(3):361-370.e3. doi: 10.1016/j.devcel.2019.01.009.

**What was the impact on technology transfer?**

Nothing to report.

**What was the impact on society beyond science and technology?**

Nothing to report.

**CHANGES/PROBLEMS:**

**Changes in approach and reasons for change**

Nothing to report.

**Actual or anticipated problems or delays and actions or plans to resolve them**

Our progress on Aims 2C and 2D has been impacted by staffing changes. Our main technical staff for the project left unexpectedly in August 2018, delaying the collection of data for this part of the project. Additionally, one of the graduate students performing the analysis for this project (Taryn Gillies) completed her thesis work and graduated. However, we have now hired a new graduate student assistant (Nicholaus DeCuzzi), and are preparing to hire additional technical assistance. With our new personnel, we expect to continue progress on the remaining tasks of the grant.

**Changes that had a significant impact on expenditures**

Nothing to report.

**Significant changes in use or care of human subjects, vertebrate animals, biohazards, and/or select agents**

Nothing to report.

**Significant changes in use or care of human subjects**

Nothing to report.

**Significant changes in use or care of vertebrate animals.**

Nothing to report.

**Significant changes in use of biohazards and/or select agents**

**PRODUCTS:**

**Publications, conference papers, and presentations**
Nothing to report.

**Journal publications.**

Nothing to report

**Books or other non-periodical, one-time publications.**

Nothing to report.

**Other publications, conference papers, and presentations.**

Nothing to report.

**Website(s) or other Internet site(s)**
Nothing to report.

**Technologies or techniques**
Our detailed methodology for image and reporter signal analysis has been published in Publication #2. Updates to these techniques will be included with forthcoming publications.

**Inventions, patent applications, and/or licenses**
Nothing to report.

**Other Products**
Reporter cell lines were developed as described above, and are made available upon publication. Signal analysis software has been developed as described in our publications and is made available upon request.

## PARTICIPANTS & OTHER COLLABORATING ORGANIZATIONS

**What individuals have worked on the project?**

*Provide the following information for: (1) PDs/PIs; and (2) each person who has worked at least one person month per year on the project during the reporting period, regardless of the source of compensation (a person month equals approximately 160 hours of effort). If information is unchanged from a previous submission, provide the name only and indicate "no change."*

| | |
|---|---|
| Name: | *John Albeck* |
| Project Role: | *PI* |
| Researcher Identifier (e.g. ORCID ID): | *1234567* |
| Nearest person month worked: | 3 |
| Contribution to Project: | *Supervised all areas of research on the project, participated in data generation and analysis.* |
| Funding Support: | *N/A* |

| | |
|---|---|
| Name: | *Taryn Gillies* |
| Project Role: | *Graduate Research Assistant* |
| Researcher Identifier (e.g. ORCID ID): | |
| Nearest person month worked: | *7* |
| Contribution to Project: | *Developed signal analysis methods for application to ERK and Akt signals; constructed cell lines and performed microscopy experiments* |
| Funding Support: | *This award* |

| | |
|---|---|
| Name: | *Heather Blizard* |
| Project Role: | *PI* |
| Researcher Identifier (e.g. ORCID ID): | |
| Nearest person month worked: | *3* |
| Contribution to Project: | *Maintained cell cultures, generated DNA constructs, developed reporter cells and cell lines; prepared frozen cell stocks* |
| Funding Support: | *This award* |

| | |
|---|---|
| Name: | *Michael Pargett* |
| Project Role: | *Postdoctoral Associate* |
| Researcher Identifier (e.g. ORCID ID): | |
| Nearest person month worked: | *6* |
| Contribution to Project: | *Developed, maintained, and debugged image analysis software; developed signal analysis techniques; performed data analysis* |
| Funding Support: | *This award and National Institutes of Health* |

| | |
|---|---|
| Name: | *Nicholaus DeCuzzi* |
| Project Role: | *Graduate Research Assistant* |
| Researcher Identifier (e.g. ORCID ID): | |
| Nearest person month worked: | *2* |
| Contribution to Project: | *Performed cell culture and microscopy experiments* |
| Funding Support: | *This award and National Institutes of Health* |

**Has there been a change in the active other support of the PD/PI(s) or senior/key personnel since the last reporting period?**

No

**What other organizations were involved as partners?**

- **Organization Name:** University of California, San Francisco
- **Location of Organization:** San Francisco, CA
- **Partner's contribution to the projec**t:

  **Collaboration** Wild type H, K, or N-Ras, mutant K-Ras, and NF1-deficient mouse fibroblasts were obtained from Dr. Frank McCormick. Dr. McCormick and Dr. Jillian Silva contributed to discussions of experimental planning and data interpretation.

## SPECIAL REPORTING REQUIREMENTS

Nothing to report.

## APPENDICES

A manuscript in preparation is attached.

## LITERATURE CITED


Courtois-Cox, S., Genther Williams, S.M., Reczek, E.E., Johnson, B.W., McGillicuddy, L.T., Johannessen, C.M., Hollstein, P.E., MacCollin, M., and Cichowski, K. (2006). A negative feedback signaling network underlies oncogene-induced senescence. Cancer Cell *10*, 459-472.

Gillies, T.E., Pargett, M., Minguet, M., Davies, A.E., and Albeck, J.G. (2017). Linear Integration of ERK Activity Predominates over Persistence Detection in Fra-1 Regulation. Cell Syst.

Gremer, L., Merbitz-Zahradnik, T., Dvorsky, R., Cirstea, I.C., Kratz, C.P., Zenker, M., Wittinghofer, A., and Ahmadian, M.R. (2011). Germline KRAS mutations cause aberrant biochemical and physical properties leading to developmental disorders. Hum Mutat *32*, 33-43.

Hunter, J.C., Manandhar, A., Carrasco, M.A., Gurbani, D., Gondi, S., and Westover, K.D. (2015). Biochemical and Structural Analysis of Common Cancer-Associated KRAS Mutations. Mol Cancer Res *13*, 1325-1335.

Konishi, H., Karakas, B., Abukhdeir, A.M., Lauring, J., Gustin, J.P., Garay, J.P., Konishi, Y., Gallmeier, E., Bachman, K.E., and Park, B.H. (2007). Knock-in of mutant K-ras in nontumorigenic human epithelial cells as a new model for studying K-ras mediated transformation. Cancer Res *67*, 8460-8467.

Omerovic, J., Hammond, D.E., Clague, M.J., and Prior, I.A. (2008). Ras isoform abundance and signalling in human cancer cell lines. Oncogene *27*, 2754-2762.

Park, K.S., Jeon, S.H., Kim, S.E., Bahk, Y.Y., Holmen, S.L., Williams, B.O., Chung, K.C., Surh, Y.J., and Choi, K.Y. (2006). APC inhibits ERK pathway activation and cellular proliferation induced by RAS. J Cell Sci *119*, 819-827.

Smith, M.J., Neel, B.G., and Ikura, M. (2013). NMR-based functional profiling of RASopathies and oncogenic RAS mutations. Proc Natl Acad Sci U S A *110*, 4574-4579.

Tuveson, D.A., Shaw, A.T., Willis, N.A., Silver, D.P., Jackson, E.L., Chang, S., Mercer, K.L., Grochow, R., Hock, H., Crowley, D., *et al.* (2004). Endogenous oncogenic K-ras(G12D) stimulates proliferation and widespread neoplastic and developmental defects. Cancer Cell *5*, 375-387.

Yeh, J.J., Routh, E.D., Rubinas, T., Peacock, J., Martin, T.D., Shen, X.J., Sandler, R.S., Kim, H.J., Keku, T.O., and Der, C.J. (2009). KRAS/BRAF mutation status and ERK1/2 activation as biomarkers for MEK1/2 inhibitor therapy in colorectal cancer. Mol Cancer Ther *8*, 834-843.

# Rescaling of oncogenic mutant Ras signals by the ERK/MAPK pathway

Taryn E. Gillies[1*], Michael Pargett[1*], Jillian M. Silva[2], Carolyn Teragawa[1], Frank McCormick[2,3], and John G. Albeck[1]

[1] Department of Molecular and Cellular Biology, University of California, Davis, CA

[2] UCSF Helen Diller Family Comprehensive Cancer Center, San Francisco, CA

[3]Frederick National Laboratory for Cancer Research, Frederick, MD, USA

[*]Equal contributions

## Abstract

Though activating mutations in Ras are present in ~30% of human tumors, the quantitative effects of these mutations on effector pathway signaling remain uncertain, with activating Ras mutants linked to both increased and decreased ERK activation. As pathway-specific treatment strategies rely on activity estimates at the cellular level, it is increasingly crucial to clarify the specific effects of Ras mutation on downstream pathways. Here, we characterize these effects for oncogenic Ras mutations at the single-cell level, using live-cell imaging with an ERK kinase activity sensor in cell lines expressing only one Ras isoform. We find that oncogenic Ras mutations restrict the range of ERK output, with elevated ERK kinase activity only in the absence of growth factor stimulus. Individual cells with mutant Ras proteins are variably responsive to acute growth factor stimulation, but do not exceed the peak magnitude of the wild type. Overall, pathway-level effects including loss of responsiveness, variable negative feedback strength, and ERK substrate-level phosphatase activity serve to sharply attenuate changes in ERK activation, relative to the magnitude of changes in Ras biochemical properties. This systematic study reconciles seemingly inconsistent reports within the literature and implies that the initial signaling changes induced by Ras mutations in oncogenesis are inherently subtle.

**Introduction**

The Ras GTPases act as molecular switches, alternating between an inactive GDP-bound state and an active GTP-bound state. In the active state, Ras proteins have increased binding affinity for their effectors (>600-fold (Gremer et al., 2011)), which are involved in multiple essential signaling pathways, including Raf/MEK/ERK and PI3K/Akt. The net signaling activity of Ras represents a balance between two classes of proteins: GTPase-Activating Proteins (GAPs), which inactivate Ras by increasing its GTPase activity, and Guanine nucleotide Exchange Factors (GEFs), which catalyze the removal of GDP and return Ras to the active GTP-bound state. Though Ras proteins are considered binary switches on the molecular level, the collective behavior of the thousands of Ras proteins present inside each cell is analogue in nature. The activation of GAPs vs. GEFs in the cell alters the fraction of Ras molecules in the active state, and the aggregate activity of Ras proteins is interpreted by downstream processes in the cell.

The three main Ras isoforms, H-Ras, K-Ras, and N-Ras, are highly similar, sharing ~90% sequence identity in the catalytic region, and differ primarily in the C-terminal “hypervariable” region, which receives posttranslational modifications necessary for membrane association. Differential modifications are implicated to target isoforms to be distributed differently across membranes, especially the plasma membrane, Golgi apparatus and endoplasmic reticulum (Prior et al., 2012). All three isoforms are expressed ubiquitously in mammalian cells, with only the K-Ras locus being necessary and sufficient for development (Esteban et al., 2001; Johnson et al., 1997; Koera et al., 1997). The function of different isoforms overlap, but incompletely, as substitution of the H-Ras sequence into the K-Ras locus permits development in mice, but yields cardiac defects in adulthood (Potenza et al., 2005).

Mutations in Ras are associated with ~30% of human cancers, especially those of the pancreas, lung, or colon (Fernandez-Medarde and Santos, 2011), and have been implicated as drivers of metastasis and poor prognosis (Yaeger et al., 2015). The majority of oncogenic mutations (86%) occur in the K-Ras isoform, with 11% in N-Ras and 3% in H-Ras. Across all isoforms, 98% of oncogenic mutations are located at the active site residues G12, G13 and Q61 (Prior et al., 2012). These mutations render the Ras proteins GAP-insensitive to varying degrees (increasing the fraction in the GTP-bound active state) and alter the binding affinity to effectors (Gremer et al., 2011; Hunter et al., 2015; Smith et al., 2013). The primary downstream effector of active Ras is

the ERK/MAPK pathway, a three-tier kinase cascade consisting of Raf, MEK and ERK, which has hundreds of downstream targets (Yoon and Seger, 2006).

Surprisingly, the mutational status of Ras is poorly correlated with average phospho-ERK levels in both tumor cell lines (Omerovic et al., 2008; Yeh et al., 2009) and in genetically engineered mouse models (Tuveson et al., 2004). Counter-intuitively, conversion of a wild type Ras gene to a mutant can *reduce* average ERK activation (Tuveson et al., 2004). Ectopic expression of Ras mutants, however, can drive strong over-activation of ERK (Konishi et al., 2007; Park et al., 2006), as expected. There are several potential explanations for these paradoxical effects: interactions with wild type Ras isoforms, effects of additional mutations in cancer cell lines, feedback-mediated changes in the Ras/ERK pathway or in its effector substrates, heterogeneous behavior across single cells, and/or limitations in resolving differences experimentally. Moreover, perturbation of Ras (or any other pathway component) may alter single-cell kinetics, such as the rate of response to growth factor or attenuation after a stimulus (Coyle and Lim, 2016), but these changes may be undetectable in population assays (Birtwistle et al., 2012; Purvis and Lahav, 2013), which have been employed almost exclusively to date.

Network feedback has particular potential to modulate signaling activity, and is a prominent feature of Ras/ERK signaling. Several layers of regulation are present and may be relevant, each capable of constraining or modulating pathway activation. First, ERK is known to directly phosphorylate and inhibit activity at several points in the pathway, including the EGFR receptor (Wells et al., 1990), the Ras GEF SOS (Langlois et al., 1995), Raf (Brummer et al., 2003; Dougherty et al., 2005), and MEK (Pages et al., 1994). Negative feedback is also evidenced via induction of phosphatase activity, which can deactivate Raf, MEK, and ERK, as well as ERK substrates (Amit et al., 2007; Brondello et al., 1997; Brondello et al., 1999). These negative feedback loops are poised to moderate activating Ras mutations, but the significance of these effects, and whether kinetics are affected, remains unclear. The landscape is further complicated by known positive feedback effects, including cooperative activation of SOS (Boykevisch et al., 2006; Margarit et al., 2003), removal of competitive inhibitors (Shin et al., 2009), inhibition of phosphatases (Marchetti et al., 2005), and stimulation of Raf (Balan et al., 2006). These interactions may modulate kinetics, generate sharper responses, or balance negative feedback. If the feedback structure does not prevent it, saturation of any of the pathway components (i.e. complete activation of all Raf, MEK or ERK molecules) represents an upper limit of ERK activation, which

would then be regulated at the level of expression. Lastly, negative regulation may also be present at the level of ERK substrates; the phosphorylation status of ERK targets is the result of competition between ERK activity and the activity of phosphatases compatible with that substrate. Measurements of active ERK concentration (i.e., dually phosphorylated ERK level) do not capture competing phosphatase activity, and may not accurately reflect some substrate phosphorylation levels. Genetically encoded kinase biosensors, however, are synthetic substrates that respond to the balance between the kinase and the competing phosphatases.

To separate the sources of variance and better resolve the effects of Ras mutation on ERK pathway output, we examined cell lines expressing wild type or mutant Ras, one isoform at a time, in an isogenic background. A Ras knockout mouse embryonic fibroblast (MEF) line which does not express H-, K-, or N-Ras was previously developed, allowing for isolated exogenous expression of single Ras isoforms (Drosten et al., 2010). These Ras knockout cells are defective in proliferation and motility, both of which are restored by expression of one Ras protein isoform from an unregulated viral promoter. In these cells, we can monitor the phosphorylation and substrate activity of ERK as driven by each isolated Ras isoform, without contribution from transcriptional regulation and with minimal background genetic differences. To comprehensively analyze single-cell kinetics of Ras/ERK signaling and the status of the whole pathway, we collected a dataset of protein expression, ERK activation (via phospho-ERK level), and ERK substrate activation (via EKAR3, a genetically encoded ERK activity sensor), in the absence and presence of stimulation by growth factors. We present a comprehensive analysis of this dataset to identify, for each mutant isoform, statistically relevant signaling differences at the average and single-cell levels, evaluate the strength and effects of feedback within the pathway, and construct a refined model of the pathway-modulated effects of altered Ras function.

## Results

### Live-cell measurements of signaling downstream from individual Ras isoforms

To evaluate the cellular signaling capacity of each Ras isoform individually, we utilized a panel of genetically engineered MEFs in which all three Ras isoforms have been knocked out and replaced with a single constitutively expressed Ras isoform (Drosten et al., 2010)(Fig. 1A). This cell line panel enabled us to characterize the signaling behavior of each Ras protein in isolation from other isoforms and from variations in transcriptional regulation. To track Ras signaling activity with high temporal resolution, we transfected each MEF cell line with EKAR3, a live-cell Förster Resonance Energy Transfer (FRET)-based ERK Activity Reporter (Harvey et al., 2008; Sparta et al., 2015) (Fig. 1B). To facilitate image segmentation, the reporter was localized to the nucleus with a C-terminal nuclear localization signal. A custom image analysis pipeline was used to perform segmentation and quantification (see Methods), typically yielding 100-300 single-cell time series measurements of ERK activity from each replicate of an experimental condition.

The signal from the EKAR reporter was derived from the intensity ratio of the cyan and yellow fluorescent channels (CFP/YFP) and corrected for background as well as excitation and filter spectra. The corrected EKAR signal linearly reflects the fraction of reporter molecules in a “FRET” conformation, which is in turn linearly related to fraction of molecules phosphorylated by ERK. Control for pathway-independent ERK activity was performed by treatment with the highly specific MEK inhibitor PD0325901 (MEKi), which rapidly inhibited the EKAR signal in all cell lines. In all live-cell experiments, MEKi treatment was used to establish the cell-specific residual EKAR signal (including the presence of non-functional reporters, a common artifact, see STAR Methods). To fully calibrate the reporter, we used Phos-Tag western blotting to quantify the fraction of the EKAR reporter that is phosphorylated in various samples and conditions (Fig. 1D), and fit these values against the average corrected EKAR signal for the same cell lines and conditions. In concert with a standard model of substrate phosphorylation, this calibration yields a linear measure of the ERK:phosphatase ratio (Fig. 1E), i.e. the concentration of active ERK divided by the concentration of active phosphatases that dephosphorylate the reporter. As these competing phosphatases also have affinity to endogenous ERK targets, the ERK activity reflects not just the levels of active ERK, but the *net* effect on substrates. See STAR Methods for the derivation of the ERK activity measurement, and calibration details.

To control for receptor-mediated ERK activity contributions via Ras-independent pathways, we included an H/K/N-Ras knock out MEF line expressing the oncogenic BRaf mutant V600E. This cell line is able to proliferate without Ras expression due to the elevated ERK activity induced by the BRaf mutant. We stimulated this cell line, along with the mutant and wild type Ras MEFs, with a panel of 6 growth factors known to activate ERK signaling (EGF, IGF, FGF, HGF, PDGF, and Amphiregulin). Three doses of each growth factor were tested across three biological replicates, yielding activity "traces" from approximately 400 cells per condition (Fig. 2A). ERK kinetics differed depending on the stimulated receptor. For example, FGF induced sustained ERK activity without pulsatile behavior, while IGF induced a single ERK activity pulse, approximately 30-40 minutes in duration, immediately following stimulation in the majority of cells.

Both FGF and IGF also induced elevated ERK in the Rasless BRaf V600E cells (Fig. 2B), indicating activity that is not solely mediated via Ras. EGF induced high amplitude ERK activity in both mutant and wild type cells, without evidence of Ras-independent activity in the BRaf cell line. The remaining growth factors, PDGF, HGF, and Amphiregulin induced transient ERK response in the wild type and mutant Ras cells. Because EGF induces a strong ERK response without Ras-independent effects, the bulk of our analysis focuses on EGF-stimulated conditions. As a final validation, the specificity of the reporter cell panel to the Ras isoforms intended was verified by treatment with ARS-853, an inhibitor specific to Ras G12C. Following treatment with ARS-853, ERK activity decreased over the course of 60 minutes in G12C MEFs, but not other Ras-MEF lines (Fig. 2C).

From each single-cell normalized ERK activity trace, we calculated baseline activity and metrics characterizing the response to stimulus: peak value, duration, mean, and mean derivative (an indicator of fluctuation over time). We statistically compared these metrics across cell types using Student's t-test, controlled for false discovery rate. Within single-cell measurements, we observe both cell-to-cell variance as well as variance among replicate experiments, with variance from replicate experiments being the greater of the two. We therefore include the cell-to-cell variance when calculating statistics, by estimating the standard error of the mean for each experimental replicate, according to a linear error model (see Methods for details). In this way, we account for variance that arises from differences in plating and growth conditions, which generates systematic biases in single-cell samples.

**The effects of Ras isoform and mutation on the growth factor response**

We first used our experimental platform to address the question of how the Ras proteins isoforms differ in their ERK signaling, especially in responses to growth factor stimuli. Cells were first incubated in growth factor-free media for 16-24 hours, followed by time-lapse imaging at 6 minute intervals, during which a stimulus of either media alone, or media with EGF (10 ng/mL final) was introduced (Fig. 3A,B). To statistically compare responses across single cells, we decomposed each single cell trace into parameters: average baseline (pre-stimulus) activity and mean absolute derivative, peak stimulated activity, amplitude, and average steady state activity. The mean derivative provides an unbiased metric of fluctuation over time, by summing the cumulative change in the signal, reflecting both frequency and amplitude without the need to classify pulses.

Under baseline conditions (pre-stimulus and mock stimulus), ERK activity varied significantly with the Ras isoform expressed (Fig. 3A-D). All mutant cell lines, as well as H-Ras, exhibited significantly elevated baseline ERK activity compared to K-Ras, with the highest levels for Q61R and G13C. In single cell activity at baseline, mutant isoforms led to less variation in ERK activity over time than the wild type, indicated by significantly diminished scaled mean derivative (Fig. 3E). Additional analysis of dynamic activity in wild type isoforms under low doses of EGF indicated minimal differences between H-, K- and N-Ras (see Supplemental Figure S1). These differences are consistent with constitutively higher GTP loading of these GTPase-deficient Ras proteins, and in the case of the BRaf cells, the insulation of the MAPK cascade from many external signals due to the lack of a Ras protein.

When stimulated, single cell responses were robust and reflected by the mean, though mutant lines exhibited more variation from cell-to-cell. EGF stimulation initiates a rapid ERK activity peak followed by attenuation (Fig. 3B,C). On average, ERK activity peaked ~15 minutes after stimulation, and decayed to an steady state level by 1.5 – 2 hours after stimulation. H- and N-Ras exhibited slower attenuation than any of the K-Ras isoforms. Despite the increased baseline signaling seen in Ras mutants, the average peak ERK activities reached after stimulation were lower than for wild-type K-Ras cells (Fig. 3B,C). Examination of single cell data revealed a potential bias in the average: the percentage of cells with a detectable ERK response was greatly reduced in mutant lines (Fig. 3F,G). Q61R in particular exhibited drastically reduced response rates, and very few BRafV600E cells responded. However, this small fraction of BRafV600E cells generated apparently genuine ERK activity responses, suggesting some involvement of a growth factor-independent

mechanism (Fig. 3G, Supplemental Fig. S2). To determine if reduced response detection could simply be attributed to smaller amplitudes as the baseline activity increases, we assessed correlation with baseline activity. While the response rate does vary with average baseline activity (Fig. 3H), correlation at the single cell level is quite poor (Fig. 3I,J); many high baseline cells clearly respond and many low baseline cells do not, regardless of cell line. Thus, the population-averaged peak ERK activity is reduced in mutant cells by a lowered response probability unrelated to current ERK activity.

Accordingly, to evaluate characteristics of actual responses, we filtered the ERK activity dataset and used only traces with a distinguishable response (Fig. 3K-M). In responding cells, the peak responses in mutant cells were equivalent to or less than in wild types (Fig. 3K). At steady state, only N-Ras and G12V drove significantly higher activity than K-Ras (Fig. 3L), though the former can be attributed to slower decay of the peak activity (Fig. 3B). This alignment at the single cell level across mutations and cloned cell lines implies that the upper range of ERK activity is subject to tight regulation. At the level of individual cells, responses varied widely (Fig. 3C, Supplemental Fig. S3) indicating either cell-specific regulation or noise. However, the immediate growth factor response, when it occurs, appears consistent, as the kinetic rate (measured as the time from stimulation to peak activity), is indistinguishable across cell lines with the current sampling (Fig. 3M). While some nuances have been identifiable, it is striking that the only sizable distinction between wild type and mutant Ras isoforms is moderate elevation of unstimulated activity.

**The range of ERK activity is maintained independently of pathway expression and Ras activity**

The restriction of hyperactive Ras mutants to only moderate changes in unstimulated ERK activity is inconsistent with naïve expectations, though it corroborates studies observing equivalent or lower phospho-ERK levels under Ras mutation (Konishi et al., 2007; Tuveson et al., 2004). Both expression level and activity of the pathway components may be compensating for differences in Ras activity. To evaluate the involvement of expression levels, we assayed average expression of pathway components, as well as ERK phosphorylation via western blot at baseline, peak (~15 minutes) and steady state (~2 hours) following a 10 ng/mL EGF stimulus.

The levels of exogenously expressed Ras isoforms varied across cell lines. Compared with the wild type K-Ras cells, Ras levels were higher in G12C and G12V lines, lower in H-Ras, and as expected, negligible

in BRafV600E (Fig. 4A). Levels of BRaf, MEK and ERK, but not CRaf, varied significantly among cell lines, without an obvious pattern or correlation structure. Some differences may be related to ERK activity via feedback; B-Raf, for example, contains a phosphodegron motif (Hernandez et al., 2016) expected to destabilize it in response to ERK activity, though this effect is not significant with current sampling.

Average ERK phosphorylation status was measured by Phos-Tag western blot. At baseline, phospho-ERK is elevated in Ras mutant cells, correlating with ERK activity measurements. In most lines, EGF produced a peak phospho-ERK (in both fraction phosphorylated and final concentration), which was diminished in the steady state (Fig. 4B,C). The peak and steady state phospho-ERK levels are significantly lower in mutant cell lines, compared to the wild type K-Ras, though it is unclear *a priori* what variation would be expected based on the Ras mutants used and relative expression levels.

To quantitatively assess how the phospho-ERK measurements differ from simple expectations of Ras-driven activity, we constructed a “naïve” mathematical model (Fig. 4D), which incorporates pathway expression levels (this study) as well as biochemical activity of Ras mutants (Gremer et al., 2011; Hunter et al., 2015; Smith et al., 2013), but does not model feedback regulation (see STAR Methods for details). This model indicates the ERK output that would be expected from the known differences in Ras isoforms (i.e. rate of GTP exchange and hydrolysis, affinity for Raf). Using a steady state solution of the naïve model, we predicted the baseline and steady state levels of phospho-ERK for each mutant cell line (Fig. 4E). Experimentally measured phospho-ERK is much lower in Ras mutants than predicted, especially at baseline. Conversely, the amplitude (fold change) in ERK with stimulation is greater in the real system than the naïve model, save for Q61R where differences are indistinguishable. Based on this comparison, the feedback regulation not included in the model effectively suppresses ppERK, but also potentially amplifies the response to growth factor stimulation.

To determine how individual expression levels contribute to phospho-ERK levels, we employed partial least square regression (PLSR), fitting phospho-ERK against the levels of each pathway member and the presence of stimulation. The PLSR was repeated for the naïve model predictions of phospho-ERK to compare dependencies with and without feedback regulation. Both experimental and naive model phospho-ERK are correlated to expression and stimulation (Fig. 4F), and as expected less of the experimental variance is explained than for the naïve model (Fig. 4G). While modeled phospho-ERK was predominantly correlated with expression of Ras, MEK and ERK, experimental phospho-ERK was significantly correlated only with the

presence of stimulation (Fig. 4G,H). We can therefore conclude that the unmodeled regulation in the pathway also provides robustness to expression level variation.

**The function of ERK-mediated feedback in Ras mutants**

To evaluate the role of ERK-mediated feedback in controlling mutant Ras output, we performed western blotting in the presence and absence of the ERK inhibitor SCH772984 (hereafter SCH), at a concentration sufficient to eliminate X% of ERK activity as measured by FRET. As this inhibitor acts as an ATP competitive inhibitor with an allosteric mode, it uncouples ERK phosphorylation from both the activity of ERK and the upstream kinase MEK (Chaikuad et al., 2014). However, MEK phosphorylation increased under both resting and EGF-stimulated conditions in wild type KRas cells (Fig. 5A), demonstrating that the negative effect exerted by active ERK on pathway activity upstream of MEK can be detected using this strategy. The 2.5-fold increase in phospho-MEK induced by SCH in the absence of growth factor stimulation occurred in the absence of an increase in GTP-bound Ras, and can be attributed to blockade of negative ERK-mediated phosphorylation of Raf. Under growth factor treatment, SCH induced a larger 4-fold increase in both phospho-MEK (at both peak and steady state) and in phospho-Akt, along with a 2-fold increase in Ras-GTP. Activating phosphorylation of EGFR at Tyr1068 was not elevated under SCH treatment, implying ERK-mediated negative feedback acting downstream of receptor kinase activity, but upstream of Ras GTP loading and activation of PI3K by Ras. Thus, ERK-mediated negative feedback operates at multiple points to constrain the output of the pathway.

In mutant KRas G12C (Fig. 5B) and Q61R (Fig. 5C), SCH produced similar effects on MEK phosphorylation, indicating that ERK-mediated negative feedback also constrains the MAPK cascade within these cells. However, the magnitude of this effect was diminished, commensurate with the expectation that the baseline phospho-MEK levels would be greater than in the wild type. SCH elevated phospho-MEK in resting cells by 1.5 and 1.7 fold respectively in G12C and Q61R cells. Under EGF stimulation, SCH increased phospho-MEK responses by <1.5 fold at peak, and by <1.7-fold at steady state. These effects can be explained by a much weaker induction of GTP-Ras, consistent with its expected constitutive loading. In G12C cells GTP loading is expect to range from 60% at baseline, to 93% when stimulated, a ~1.5-fold change; in the assay, GTP-Ras was stimulated by only 1.2-fold by EGF treatment, and this response was not significantly

enhanced by SCH. In Q61R, which has been shown to be close to fully GTP-bound even in the absence of growth factor (97% at baseline to 99% with stimulation), GTP-Ras decreased in response to both GF and SCH, an effect that may be related to competition of endogenous GEFs in the RBD pulldown assay. A strong phospho-EGFR and phospho-Akt response to GF in both of these cells, irrespective of SCH treatment, confirmed that the responsiveness of the receptor remained intact. Two major conclusions can be drawn from these data: 1) that ERK-mediated feedback restrains pathway output in both wild type and mutant Ras contexts, both before and during GF stimulus, and 2) that the signal range (fold-change on stimulation) is amplified at the level of phospho-MEK, as both GF- and SCH-dependent changes in MEK phosphorylation are large relative to those detectable in GTP-Ras.

**Phosphatases dynamically shape the functional ERK output**

It is striking that stimulated ERK activity was nearly consistent across cell lines, but phospho-ERK level varied; this difference implicates variation in phosphatase activity, as the only variable theoretically separating our measurements of ERK phosphorylation and activity. Comparing the ERK activity and phospho-ERK averages for each cell line and time point, a significant linear relationship is evidenced among cell lines at baseline, implying near constant phosphatase activities (Fig. 6A). However, while stimulation increases both phospho-ERK and ERK activity, their correlation across cell lines is progressively diminished at the peak and steady state time points. This change implies that phosphatase activity may be coordinated to maintain a target level of stimulated ERK activity.

To clarify the impact of phosphatases, we estimated the substrate phosphatase activity as the ratio of ppERK to ERK activity averaged over all replicates for each cell line and time point (Fig. 6B). Phosphatase activity is nearly uniform at baseline, with KRas as a notable outlier without explanation; the effect could reflect an isoform-specific function, or merely the nature of the single cloned K-Ras cell line. As the inverse of the view in Fig. 6A, phosphatase activity varies among cell lines after stimulation, increasingly correlated with ppERK over time. This behavior implies some involvement of feedforward control from growth factor stimulation, as phosphatase activity is not always correlated to ppERK, only after stimulation. The phosphatase response further evidences a coherent dynamic pattern following stimulation, with a significant rise in activity between peak and steady state times ($p = 0.005$), accounting for (42% - 73% of) the drop in ERK activity after

1 hour of stimulation. These analyses support a model where phosphatase activity sharpens the growth factor response and normalizes stimulated ERK activity levels, potentially being immediately inhibited but stimulated after a delay, thus suppressing steady state ERK activity.

## Discussion

*Mechanisms constraining the range of mutant Ras signaling*

The Ras/ERK signaling pathway is both a focal point for disease-causing mutations and a model for systems-level functions of signaling pathways. However, the flexibility of the pathway, and the complex genetics of cancer, have limited our understanding of how the magnitude of pathway output is determined (Fey et al., 2016). Here, we investigate the interaction between disease-associated Ras mutants and pathway flexibility within a single, genetically simplified system, with the goal of providing a unified model for why changes in Ras protein activity do not consistently result in corresponding activation of ERK. Our results identify multiple layers of regulation that act to both enhance and suppress ERK responses downstream of Ras mutants, with the net effect that changes in ERK activation are greatly restricted relative to the biochemical properties of mutant Ras proteins. While in some pathways output can be fine-tuned by shifts in expression level (Gaudet et al., 2012), our measurements indicate that the Ras/ERK pathway exhibits robustness to pathway expression levels and biochemical properties of Ras, and that response output is primarily regulated at the level of kinase activity. Conceptually, these constraints on signal intensity are similar to dose response alignment (Yu et al., 2008) and adaptive effects found in yeast MAPK cascades (Muzzey et al., 2009). Our study uniquely demonstrates that these pathway-level mechanisms shape the functional output of pathological mutations.

The physiological function of the EGFR/Ras/ERK pathway depends on its ability to distinguish between different stimulation states – the absence of EGF, the arrival of a new EGF stimulus, and steady state EGF stimulation (Fig. 7). While it is clear that cancer cells have an altered perception of these states (Bugaj et al., 2018), it is less obvious precisely how this alteration arises from specific molecular changes in disease. Experimental models of the conversion of a single K-Ras allele from wild-type to GTPase-defective mutant (the essential first step in Ras-mediated oncogenesis) have reached the consensus that this alteration creates a very limited shift in signaling behavior, but differ in conclusions regarding the magnitude of ERK activation and whether or not it requires stimulus (Guerra et al., 2003; Huang et al., 2014; Konishi et al., 2007; Tuveson et al., 2004). Many of these differences can now be attributed to the temporal and quantitative limitations of the methods previously used to track ERK activation (primarily uncalibrated phospho-ERK immunoblots). Our dataset recapitulates most of the reported attributes of mutant Ras signaling, which in isolation appear

contradictory, including elevated baseline signaling, reduced absolute peak height upon initial stimulus, and maintenance of the capacity for GF stimulation. The ability to resolve these differences with self-consistent, calibrated FRET measurements and matched immunoblots underscores the importance of a quantitative, systematic approach to complex signaling networks

While it has been suggested that suppression of ERK in mutant Ras cells results mainly from negative feedback from ERK (Courtois-Cox et al., 2006), our systematic analysis reveals a more complex situation with multiple contributing factors. ERK-mediated negative feedback does play a role in restraining MEK activation, but it does so to a lesser extent in mutant Ras cells than in wild type (Fig. 5). Instead, we find that Ras-mutant cells have a reduced probability of response that is independent of their current ERK activity and contributes to a lower pERK signal on immunoblots (in which all cells are averaged). Yet, even when this effect is accounted for in single cells, ERK responses remain limited in amplitude in Ras-mutant cells. One model for this diminished response is that the Raf/MEK/ERK cascade acts as fold-change detector for variation in Ras-GTP. Because a higher fraction of mutant Ras is GTP-bound prior to stimulus, the fold change in Ras-GTP achievable by GF stimulation is smaller than in wild type (see Fig. 5, and (Patricelli et al., 2016), which would lead to a smaller MEK/ERK response. In this model, pathway-level negative feedback mediated by ERK activity plays a complex role – it restrains the excessive signal intensity generated mutant Ras, but also preserves the ability of the pathway to respond to growth factor stimulus, enhancing the amplitude of growth factor responses.

In addition to negative feedback, we identify several other factors that contribute to making ERK activity in mutant Ras cells more responsive to growth factors than would be expected based on their constitutively high GTP loading status of Ras. One is the capacity for Ras-independent growth factor stimulation of ERK, which is minimal for EGF stimulation, but substantial for several other growth factors (Fig. 2). While protein kinase C (PKC) is a potential route for this signal, we were unable to block the increase using PKC inhibitors (data not shown). In a physiological context, this would further preserve normal growth factor responses. Another, more unexpected, factor is the apparent fine-tuning of phosphatase activity acting on ERK substrates, which decreases systematically in K-Ras mutants relative to wild type K-Ras. As ERK phosphorylation is often used as the *de facto* measurement for its activity, quantitative effects at the level of substrates have received less attention. Nonetheless, the ability of ERK to maintain phosphorylation of its substrates is inherently limited

by the opposing process of dephosphorylation, making this a critical but understudied control point. Our data imply that regulation of this process is significant for an exogenous FRET-based substrate (whose substrate sequence is based on the endogenous substrate Cdc25A), warranting further study of this effect on endogenous substrates. This effect could be mediated by control of phosphatases acting on ERK substrates, or through competition of substrates for the phosphatase; future work will be needed to elucidate this mechanism.

An additional possible normalizing factor is the opportunity for each Ras variant line to be subject to selection during the process of cell line construction and propagation. Cells receiving a Ras insertion that produces high levels of expression could be driven into senescence by excessive ERK activity, thus selecting against these individual cells. Therefore, cells bearing epigenetic modifications or point mutations that moderate the output of ERK could be overrepresented in the surviving population. While our analysis suggests that expression levels of pathway components is not a major factor determining the ERK activity of our cell lines, we cannot rule out the possibility of activity-modifying mutations that do not alter expression levels. We note that the same caveat applies to the vast majority of cell-based experiments on Ras signaling (including transient expression experiments that typically exceed at least one cell cycle). Thus, experimental strategies in which Ras isoforms are abruptly exchanged, and the resulting cellular changes monitored with high temporal resolution, could be informative in understanding the adaptation to a Ras mutation.

*Constraints on Ras-driven signaling in oncogenesis*

The ability of the MAPK pathway to constrain the quantitative effects of mutant Ras raises important questions for how these mutations function in oncogenesis. In many cancers, Ras mutations are thought to occur very early in oncogenesis, and therefore the homeostatic nature of the pathway likely plays a central role in determining whether a Ras mutant cell progresses toward malignancy (Li et al., 2018). Our data from cells with few other genetic abnormalities can be a considered a model for signaling at this early stage, unique from studies that have investigated mutant Ras in fully developed cancers and focused on treatment of later-stage disease.

How do early changes in ERK signaling drive further malignant changes to the cell? One potential model is that excess levels of ERK activity may engage lower-affinity targets, expanding the effective ERK-

driven phosphoproteome to non-traditional targets. However, given the constraints we observe on signaling, it is impractical for these Ras mutant cells to activate anything other than typical ERK targets. As mutant bearing cells do not show longer duration of ERK activity following stimulus than those with wild type Ras, excess activation of proteins sensitive to prolonged stimuli is also unlikely. Instead, the limitation of over-activating effects of Ras mutants to chronic baseline elevation implies (1) that chronic moderate signaling is sufficient to drive deleterious phenotypes, and (2) that mutant cells are unable to respond to normal low-level signaling. A strong downstream effect from chronic moderate ERK activity is consistent with current models of some effectors. The ERK target gene Fra-1, a transcription factor whose expression is correlated with cancer invasiveness (Tam et al., 2013), integrates ERK activity over time (Gillies et al 2017). With its slow decay rate (half-life > 5h, (Basbous et al., 2007)), Fra-1 can accumulate to relatively high levels after a long period of moderately elevated ERK activity. Any ERK-induced gene products with similar degradation kinetics will also accumulate over time in cells with baseline ERK elevation. Conversely, gene products subject to rapid degradation kinetics such as c-Fos and Egr-1 are likely to be only weakly elevated in Ras mutants, as even short sporadic wild type activity will drive large changes in expression. Products under negative regulation may even be suppressed by the chronic ERK activity, such as gene products that degrade rapidly even with extended activity (Wilson et al., 2017). Thus, while enhanced ERK kinase activity as an indicator of early Ras mutant cells is difficult to detect without live-cell measurements, the resulting expression profile - particularly the ratio between long-term and short-term responsive genes - may be more informative.

While the damping of mutant Ras-driven signals at the level of ERK may appear to be a tumor suppressive mechanism, this is not necessarily the case. Analysis of mutation frequencies in human cancer and data from mouse models suggests a model in which a limited quantitative range of Ras output (a “sweet spot”) is critical for the development of tumors (Li et al., 2018; Sarkisian et al., 2007). Pathway constraints could help Ras mutant cells to stay within this range and evade senescence or cell death due to excessive ERK activation. This paradox raises the question of whether Ras mutants are more common than downstream mutations (such as MEK or ERK) in cancer and related syndromes such as RASopathies because they are strong enough to induce increased ERK activity, or rather because they are selected for due to their inherently weaker and more controlled output.

**Figure Legends**

Figure 1. ERK measurement in cell lines expressing a single Ras isoform. A) Schematic of EGF signaling through Ras to ERK, including the EKAR3 sensor. B) Construction scheme for single Ras cell lines from H/K/N-Ras knockouts. C) Conceptual expectations from mutation of the only Ras isoform, including effects modulating average or peak ERK activity, or response duration. D) Sample calibration data for the EKAR3 reporter, consisting of Phos-Tag western blot for phospho-EKAR and live-cell imaging of reporter FRET activity under matched conditions for 4 cell lines. Four single nuclei from the wild type K-Ras line are shown before and after stimulus. E) Calibration curves for ERK activity. Fraction of EKAR3 phosphorylated is shown vs. the fraction in the associated conformation by FRET (left). The ERK to phosphatase ratio (right) is derived from a model of EKAR3 (see STAR Methods).

Figure 2. Activity profiles of cell lines expressing a single Ras isoform. A) Graphical summary of single Ras cell lines stimulated by a panel of growth factors. All scales are equal. Lines indicate median of single cell measurements over time, and shaded regions denote the $25^{th}$ – $75^{th}$ percentile region. B) Demonstration of Ras independent activity from ligands other than EGF, evidenced by response in the BRafV600E cell line lacking H/K/N Ras. C) Demonstration of cell line specificity via ARS-853, a Ras activity inhibitor specific to the G12C mutant.

Figure 3. ERK activity across Ras isoforms in response to EGF stimulation. A-E) ERK activity in each of the 8 cell lines, after growth factor withdrawal form 16-24 hours, followed by stimulus consisting of (A) media only, or (B) 10 ng/mL EGF. C) Three example single cell traces per cell line. D) Average baseline (pre-stimulus) ERK activity over N replicate experiments per cell line. Each dot represents the median value across cells in an experiment and lines represent the $25^{th}$ – $75^{th}$ percentiles. The red bar denotes the median across all replicates. E) Mean absolute derivative, scaled by mean value, reflecting the scale of variation over time, displayed as in D. F-J) Analysis of single-cell response likelihood after EGF stimulus. F) Demonstration of large fractions of cell not responding to EGF stimulus in some mutants. G) Likelihood of single cells responding to EGF stimulus, for each cell line. H) Relationship between response likelihood and average baseline ERK activity as a possible correlate, for each cell line. I) Weakness of correlation between baseline ERK activity and

response likelihood, measured by Tjur's coefficient of discrimination (equivalent to a correlation coefficient for the binary response). Inset shows an example from the G12D mutant, where dots are scattered per cell by baseline ERK activity (x-axis) and if that cell responded to EGF (binary y-axis). Orange line indicates the logistic fit. J) Scattered single cell measurements of baseline ERK activity and amplitude of the change after EGF stimulus, color-coded by recognition as a responding cell. K-L) Analysis of the response to EGF, by filtering to remove cells that do not respond. Dots represent median over cells in an experiment, bars denote the $25^{th}$ – $75^{th}$ percentiles and red horizontal bars show the median over replicate experiments. K) Peak ERK activity reached after EGF stimulus. L) Average ERK activity after 2 hours in the presence of EGF. M) Delay between EGF stimulus and peak ERK activity.

Figure 4. Feedback regulation of ERK phosphorylation. A) Western blot measurement of Ras-ERK pathway components in each cell line, at baseline (grey circles), peak activity (12-15 minutes, red triangles) and steady state activity (~2 hours, blue diamonds). The median and $25^{th}$ – $75^{th}$ percentiles over all conditions are indicated by overlaid whisker plots. Asterisks indicate statistical significance from the K-Ras WT cell line. Sample blot imagery is proved underneath each quantification. B-C) Phos-Tag western blot measurement of ERK fractional phosphorylation (B) and the relative concentration of dually phosphorylated ERK (C), annotated as in A, but with summary statistics per treatment condition. Sample blot imagery shows anti-ERK1/2 (B) and anti-ppERK1/2 (C) for the same blot replicate. D) Schematic of a feedback free "naïve" model of Ras-ERK activation. Shaded regions indicate portions of the model for which parameter values are available from either published biochemical assays or our western blot data. E-F) Comparison of the naïve model to experimental data. E) Relative ppERK as predicted by the naïve model and measured by western blot, showing baseline conditions, steady state after EGF treatment, and the amplitude of stimulation. F-H) Partial least squares regression of both experimental ppERK measurements and predictions via the naïve model. Regression was based on presence/absence of EGF, and expression levels of Ras, Raf, MEK and ERK. F) PLS model prediction vs. actual measurements. Black and red dots are based on experimental and naïve model data, respectively. The dashed line indicates perfect alignment. G) Percent of variance explained by each PLS model considered, based on how many component terms are allowed. Stim only refers to a PLS model using experimental ppERK data, but only predicting based on the presence/absence of EGF. H) Weights assigned to

each parameter in the PLS models. Grey lines indicate threshold values, above which the parameter weight is statistically significant from zero.

Figure 5. ERK dependent feedback in Ras mutants. A-C) Western blot analysis of Ras-ERK pathway activity at multiple levels under ERK inhibition via [dosage] SCH772984 (ERKi). Lysates for select cell lines (K-Ras WT, G12C, Q61R) are included at baseline, and peak (~15 min) and steady state (~2 hours) after treatment with 100 ng/mL EGF. Data for each cell line are normalized to the control treatment (DMSO, no ERKi) at baseline. Sample blot imagery is provide underneath each quantification. A) EGFR activation as measured by an antibody specific to phospho-Tyr1068. B) Ras-GTP level, as measured by pulldown with bead conjugated Ras binding domain (RBD). C) Phosphorylated MEK (S217 or S221), ERK (T202/Y204) and Akt (S473).

Figure 6. Effect of phosphatase regulation on ERK activity. A) Correlation of ERK activity and ppERK concentration, per condition. Markers are color-coded by cell line, and marker shape indicates treatment (circle: baseline, triangle: peak, diamond: steady state). Pearson's correlation coefficients and associated P-values are printed for each treatment. B) Estimate of substrate level phosphatase activity per cell line and treatment. Asterisk indicates significance when comparing all cell lines.

Figure 7. Consolidated model of Ras mutation effects on ERK signaling.

## STAR Methods

### Cell Culture

Mouse embryonic fibroblasts expressing a single Ras isoform were obtained from [ref]. Cells were cultured in DMEM supplemented with 0.2% bovine serum albumin (BSA) and X ng/mL puromycin or blasticidin. For imaging experiments, cells were cultured in a custom imaging media composed of DMEM lacking phenol red, folate and riboflavin, glucose, glutamine, and pyruvate, supplemented with 0.1% BSA, 4mM L-glutamine, and 25mM glucose.

### Reporter Cell Line Construction

Cells were electroporated using a Lonza Nucleofector electroporator. EKAR3 was stably integrated into cells using the piggyBAC transposase system (Pargett et al., 2017). Positive integrants were selected by fluorescence-based cell sorting.

### Live Cell Microscopy

Multi-well plates with #1.5 glass bottoms were coated with collagen and seeded with reporter cell lines one day prior to imaging. Prepared culture plates were imaged on a Nikon Ti-E inverted microscope with a stage-top incubator to maintain the culture at 37˚C and 5% CO2 throughout the experiment. Microscopy and image processing preformed as described in (Pargett et al, 2017). Imaging sites within each well were selected and imaged sequentially at each acquisition time, automated via the NIS-Elements AR software. Images were captured using a 20x/0.75 NA objective and an Andor Zyla 5.5 scMOS camera.

### Immunofluorescence Microscopy

After growth and treatment as indicated on glass-bottom 96-well plates, cells were fixed for 30 min at room temperature with a freshly prepared solution of 12% paraformaldehyde in PBS and permeabilized with 1% Triton X-100. Samples were then stained with primary and secondary antibodies in PBS+0.1% Triton X-100+2% bovine serum albumin, and images were captured on a Nikon Ti-E inverted microscope with a 20x/0.75 NA objective with an Andor Zyla 5.5 scMOS camera.

**Image Processing**

Imaging data were processed to segment and average pixels within each identified cell's nucleus and cytoplasm, using a custom procedure written for MATLAB (Pargett et al., 2017). The procedure accessed image data from ND2 files generated by NIS Elements, using the Bio-Formats MATLAB toolbox, and tracked single cell positions over time using uTrack 2.0 (Jaqaman et al., 2008). The resulting single cell time series traces were filtered for quality (minimum length of trace, maximum number of contiguous missing or corrupt data points), and ratiometric reporter levels calculated. EKAR3 level was calculated as $1 - \frac{CFP/YFP}{R_P}$, where $CFP$ and $YFP$ are the pixel intensities of the cyan and yellow channels, respectively, and $R_P$ is the ratio of total power collected in cyan over that of yellow (each computed as the spectral products of relative excitation intensity, exposure time, molar extinction coefficient, quantum yield, light source spectrum, filter transmissivities, and fluorophore absorption and emission spectra).

**Statistical Analysis**

For all experiments shown, a minimum of 100 cells were imaged and tracked for each condition. Single-cell data points were excluded as outliers if greater than six standard deviations from the dataset mean. For all analyses, at least three independent experimental replicates were performed. Where indicated, single cell data were normalized to the median value of the PD0325901-treated region. All statistical and computational tasks were performed using MATLAB.

Each single cell trace was normalized to the minimum value in a 1 hour window following treatment with 100nM PD0325901. Baseline values were calculated by taking the mean of the 3 hour window prior to stimulation for each cell. The mean was calculated from a 3.5 hour window following treatment with the specified growth factor or vehicle control. Mean derivative is calculated as the sum of the absolute value of the derivative over a 3.5 hour window following stimulation. Responders were defined as cells who's post-stimulation ERK activity increased at least 5% compared to the average baseline value, had a higher maximum derivative at the time of stimulation compared to the baseline region, and had a significantly different ($p < .05$) distribution of ERK activity values following stimulation compared to the distribution in the baseline region. Response location was defined as the time point where the cell reached its maximum ERK activity value

following stimulation in each responding cell. Duration was calculated as full width at half maximum for each responding cell.

The mean of each metric was calculated for every replicate experiment, and the distribution of these replicate means was compared for each cell line against K-Ras wild type. Each comparison was made by t-test, with false discovery rate controlled across all comparisons via the method of Benjamini and Hochberg[1]. Where replicates were available at the single cell level as well as across experiments, the standard deviation of the mean for each experiment was determined from single-cell samples and added to experimental variance. This corresponds to a linear error model: $\varepsilon_i = \varepsilon_{cell} + \varepsilon_{exp}$, where there error (from the mean) of an individual cell $\varepsilon_i$ equals the sum of the errors arising from cell-to-cell variation $\varepsilon_{cell}$ and from experiment variation $\varepsilon_{exp}$.

## References


Amit, I., Citri, A., Shay, T., Lu, Y., Katz, M., Zhang, F., Tarcic, G., Siwak, D., Lahad, J., Jacob-Hirsch, J.*, et al.* (2007). A module of negative feedback regulators defines growth factor signaling. Nat Genet *39*, 503-512.

Balan, V., Leicht, D.T., Zhu, J., Balan, K., Kaplun, A., Singh-Gupta, V., Qin, J., Ruan, H., Comb, M.J., and Tzivion, G. (2006). Identification of novel in vivo Raf-1 phosphorylation sites mediating positive feedback Raf-1 regulation by extracellular signal-regulated kinase. Mol Biol Cell *17*, 1141-1153.

Basbous, J., Chalbos, D., Hipskind, R., Jariel-Encontre, I., and Piechaczyk, M. (2007). Ubiquitin-independent proteasomal degradation of Fra-1 is antagonized by Erk1/2 pathway-mediated phosphorylation of a unique C-terminal destabilizer. Mol Cell Biol *27*, 3936-3950.

Birtwistle, M.R., Rauch, J., Kiyatkin, A., Aksamitiene, E., Dobrzynski, M., Hoek, J.B., Kolch, W., Ogunnaike, B.A., and Kholodenko, B.N. (2012). Emergence of bimodal cell population responses from the interplay between analog single-cell signaling and protein expression noise. BMC Syst Biol *6*, 109.

Boykevisch, S., Zhao, C., Sondermann, H., Philippidou, P., Halegoua, S., Kuriyan, J., and Bar-Sagi, D. (2006). Regulation of ras signaling dynamics by Sos-mediated positive feedback. Curr Biol *16*, 2173-2179.

Brondello, J.M., Brunet, A., Pouyssegur, J., and McKenzie, F.R. (1997). The dual specificity mitogen-activated protein kinase phosphatase-1 and -2 are induced by the p42/p44MAPK cascade. J Biol Chem *272*, 1368-1376.

Brondello, J.M., Pouyssegur, J., and McKenzie, F.R. (1999). Reduced MAP kinase phosphatase-1 degradation after p42/p44MAPK-dependent phosphorylation. Science *286*, 2514-2517.

Brummer, T., Naegele, H., Reth, M., and Misawa, Y. (2003). Identification of novel ERK-mediated feedback phosphorylation sites at the C-terminus of B-Raf. Oncogene *22*, 8823-8834.

Bugaj, L.J., Sabnis, A.J., Mitchell, A., Garbarino, J.E., Toettcher, J.E., Bivona, T.G., and Lim, W.A. (2018). Cancer mutations and targeted drugs can disrupt dynamic signal encoding by the Ras-Erk pathway. Science *361*.

Chaikuad, A., Tacconi, E.M.C., Zimmer, J., Liang, Y., Gray, N.S., Tarsounas, M., and Knapp, S. (2014). A unique inhibitor binding site in ERK1/2 is associated with slow binding kinetics. Nat Chem Biol *10*, 853-860.

Courtois-Cox, S., Genther Williams, S.M., Reczek, E.E., Johnson, B.W., McGillicuddy, L.T., Johannessen, C.M., Hollstein, P.E., MacCollin, M., and Cichowski, K. (2006). A negative feedback signaling network underlies oncogene-induced senescence. Cancer Cell *10*, 459-472.

Coyle, S.M., and Lim, W.A. (2016). Mapping the functional versatility and fragility of Ras GTPase signaling circuits through in vitro network reconstitution. eLife Sciences *5*, e12435.

Dougherty, M.K., Muller, J., Ritt, D.A., Zhou, M., Zhou, X.Z., Copeland, T.D., Conrads, T.P., Veenstra, T.D., Lu, K.P., and Morrison, D.K. (2005). Regulation of Raf-1 by direct feedback phosphorylation. Mol Cell *17*, 215-224.

Drosten, M., Dhawahir, A., Sum, E.Y., Urosevic, J., Lechuga, C.G., Esteban, L.M., Castellano, E., Guerra, C., Santos, E., and Barbacid, M. (2010). Genetic analysis of Ras signalling pathways in cell proliferation, migration and survival. EMBO J *29*, 1091-1104.

Esteban, L.M., Vicario-Abejon, C., Fernandez-Salguero, P., Fernandez-Medarde, A., Swaminathan, N., Yienger, K., Lopez, E., Malumbres, M., McKay, R., Ward, J.M.*, et al.* (2001). Targeted genomic disruption of H-ras and N-ras, individually or in combination, reveals the dispensability of both loci for mouse growth and development. Mol Cell Biol *21*, 1444-1452.

Fernandez-Medarde, A., and Santos, E. (2011). Ras in cancer and developmental diseases. Genes Cancer *2*, 344-358.

Fey, D., Matallanas, D., Rauch, J., Rukhlenko, O.S., and Kholodenko, B.N. (2016). The complexities and versatility of the RAS-to-ERK signalling system in normal and cancer cells. Semin Cell Dev Biol *58*, 96-107.

Gaudet, S., Spencer, S.L., Chen, W.W., and Sorger, P.K. (2012). Exploring the contextual sensitivity of factors that determine cell-to-cell variability in receptor-mediated apoptosis. PLoS Comput Biol *8*, e1002482.

Gremer, L., Merbitz-Zahradnik, T., Dvorsky, R., Cirstea, I.C., Kratz, C.P., Zenker, M., Wittinghofer, A., and Ahmadian, M.R. (2011). Germline KRAS mutations cause aberrant biochemical and physical properties leading to developmental disorders. Hum Mutat *32*, 33-43.

Guerra, C., Mijimolle, N., Dhawahir, A., Dubus, P., Barradas, M., Serrano, M., Campuzano, V., and Barbacid, M. (2003). Tumor induction by an endogenous K-ras oncogene is highly dependent on cellular context. Cancer Cell *4*, 111-120.

Harvey, C.D., Ehrhardt, A.G., Cellurale, C., Zhong, H., Yasuda, R., Davis, R.J., and Svoboda, K. (2008). A genetically encoded fluorescent sensor of ERK activity. Proc Natl Acad Sci U S A *105*, 19264-19269.

Hernandez, M.A., Patel, B., Hey, F., Giblett, S., Davis, H., and Pritchard, C. (2016). Regulation of BRAF protein stability by a negative feedback loop involving the MEK-ERK pathway but not the FBXW7 tumour suppressor. Cell Signal *28*, 561-571.

Huang, H., Daniluk, J., Liu, Y., Chu, J., Li, Z., Ji, B., and Logsdon, C.D. (2014). Oncogenic K-Ras requires activation for enhanced activity. Oncogene *33*, 532-535.

Hunter, J.C., Manandhar, A., Carrasco, M.A., Gurbani, D., Gondi, S., and Westover, K.D. (2015). Biochemical and Structural Analysis of Common Cancer-Associated KRAS Mutations. Mol Cancer Res *13*, 1325-1335.

Johnson, L., Greenbaum, D., Cichowski, K., Mercer, K., Murphy, E., Schmitt, E., Bronson, R.T., Umanoff, H., Edelmann, W., Kucherlapati, R.*, et al.* (1997). K-ras is an essential gene in the mouse with partial functional overlap with N-ras. Genes Dev *11*, 2468-2481.

Koera, K., Nakamura, K., Nakao, K., Miyoshi, J., Toyoshima, K., Hatta, T., Otani, H., Aiba, A., and Katsuki, M. (1997). K-ras is essential for the development of the mouse embryo. Oncogene *15*, 1151-1159.

Konishi, H., Karakas, B., Abukhdeir, A.M., Lauring, J., Gustin, J.P., Garay, J.P., Konishi, Y., Gallmeier, E., Bachman, K.E., and Park, B.H. (2007). Knock-in of mutant K-ras in nontumorigenic human epithelial cells as a new model for studying K-ras mediated transformation. Cancer Res *67*, 8460-8467.

Langlois, W.J., Sasaoka, T., Saltiel, A.R., and Olefsky, J.M. (1995). Negative feedback regulation and desensitization of insulin- and epidermal growth factor-stimulated p21ras activation. J Biol Chem *270*, 25320-25323.

Li, S., Balmain, A., and Counter, C.M. (2018). A model for RAS mutation patterns in cancers: finding the sweet spot. Nat Rev Cancer *18*, 767-777.

Marchetti, S., Gimond, C., Chambard, J.C., Touboul, T., Roux, D., Pouyssegur, J., and Pages, G. (2005). Extracellular signal-regulated kinases phosphorylate mitogen-activated protein kinase phosphatase 3/DUSP6 at serines 159 and 197, two sites critical for its proteasomal degradation. Mol Cell Biol *25*, 854-864.

Margarit, S.M., Sondermann, H., Hall, B.E., Nagar, B., Hoelz, A., Pirruccello, M., Bar-Sagi, D., and Kuriyan, J. (2003). Structural evidence for feedback activation by Ras.GTP of the Ras-specific nucleotide exchange factor SOS. Cell *112*, 685-695.

Muzzey, D., Gomez-Uribe, C.A., Mettetal, J.T., and van Oudenaarden, A. (2009). A systems-level analysis of perfect adaptation in yeast osmoregulation. Cell *138*, 160-171.

Omerovic, J., Hammond, D.E., Clague, M.J., and Prior, I.A. (2008). Ras isoform abundance and signalling in human cancer cell lines. Oncogene *27*, 2754-2762.

Pages, G., Brunet, A., L'Allemain, G., and Pouyssegur, J. (1994). Constitutive mutant and putative regulatory serine phosphorylation site of mammalian MAP kinase kinase (MEK1). EMBO J *13*, 3003-3010.

Park, K.S., Jeon, S.H., Kim, S.E., Bahk, Y.Y., Holmen, S.L., Williams, B.O., Chung, K.C., Surh, Y.J., and Choi, K.Y. (2006). APC inhibits ERK pathway activation and cellular proliferation induced by RAS. J Cell Sci *119*, 819-827.

Patricelli, M.P., Janes, M.R., Li, L.-S., Hansen, R., Peters, U., Kessler, L.V., Chen, Y., Kucharski, J.M., Feng, J., Ely, T.*, et al.* (2016). Selective Inhibition of Oncogenic KRAS Output with Small Molecules Targeting the Inactive State. Cancer Discov *6*, 316-329.

Potenza, N., Vecchione, C., Notte, A., De Rienzo, A., Rosica, A., Bauer, L., Affuso, A., De Felice, M., Russo, T., Poulet, R.*, et al.* (2005). Replacement of K-Ras with H-Ras supports normal embryonic development despite inducing cardiovascular pathology in adult mice. EMBO Rep *6*, 432-437.

Prior, I.A., Lewis, P.D., and Mattos, C. (2012). A comprehensive survey of Ras mutations in cancer. Cancer Res *72*, 2457-2467.

Purvis, J.E., and Lahav, G. (2013). Encoding and decoding cellular information through signaling dynamics. Cell *152*, 945-956.

Sarkisian, C.J., Keister, B.A., Stairs, D.B., Boxer, R.B., Moody, S.E., and Chodosh, L.A. (2007). Dose-dependent oncogene-induced senescence in vivo and its evasion during mammary tumorigenesis. Nat Cell Biol *9*, 493-505.

Shin, S.Y., Rath, O., Choo, S.M., Fee, F., McFerran, B., Kolch, W., and Cho, K.H. (2009). Positive- and negative-feedback regulations coordinate the dynamic behavior of the Ras-Raf-MEK-ERK signal transduction pathway. J Cell Sci *122*, 425-435.

Smith, M.J., Neel, B.G., and Ikura, M. (2013). NMR-based functional profiling of RASopathies and oncogenic RAS mutations. Proc Natl Acad Sci U S A *110*, 4574-4579.

Sparta, B., Pargett, M., Minguet, M., Distor, K., Bell, G., and Albeck, J.G. (2015). Receptor Level Mechanisms Are Required for Epidermal Growth Factor (EGF)-stimulated Extracellular Signal-regulated Kinase (ERK) Activity Pulses. J Biol Chem *290*, 24784-24792.

Tam, W.L., Lu, H., Buikhuisen, J., Soh, B.S., Lim, E., Reinhardt, F., Wu, Z.J., Krall, J.A., Bierie, B., Guo, W.*, et al.* (2013). Protein kinase C alpha is a central signaling node and therapeutic target for breast cancer stem cells. Cancer Cell *24*, 347-364.

Tuveson, D.A., Shaw, A.T., Willis, N.A., Silver, D.P., Jackson, E.L., Chang, S., Mercer, K.L., Grochow, R., Hock, H., Crowley, D.*, et al.* (2004). Endogenous oncogenic K-ras(G12D) stimulates proliferation and widespread neoplastic and developmental defects. Cancer Cell *5*, 375-387.

Wells, A., Welsh, J.B., Lazar, C.S., Wiley, H.S., Gill, G.N., and Rosenfeld, M.G. (1990). Ligand-induced transformation by a noninternalizing epidermal growth factor receptor. Science *247*, 962-964.

Wilson, M.Z., Ravindran, P.T., Lim, W.A., and Toettcher, J.E. (2017). Tracing Information Flow from Erk to Target Gene Induction Reveals Mechanisms of Dynamic and Combinatorial Control. Mol Cell *67*, 757-769 e755.

Yaeger, R., Cowell, E., Chou, J.F., Gewirtz, A.N., Borsu, L., Vakiani, E., Solit, D.B., Rosen, N., Capanu, M., Ladanyi, M.*, et al.* (2015). RAS mutations affect pattern of metastatic spread and increase propensity for brain metastasis in colorectal cancer. Cancer *121*, 1195-1203.

Yeh, J.J., Routh, E.D., Rubinas, T., Peacock, J., Martin, T.D., Shen, X.J., Sandler, R.S., Kim, H.J., Keku, T.O., and Der, C.J. (2009). KRAS/BRAF mutation status and ERK1/2 activation as biomarkers for MEK1/2 inhibitor therapy in colorectal cancer. Mol Cancer Ther *8*, 834-843.

Yoon, S., and Seger, R. (2006). The extracellular signal-regulated kinase: multiple substrates regulate diverse cellular functions. Growth Factors *24*, 21-44.

Yu, R.C., Pesce, C.G., Colman-Lerner, A., Lok, L., Pincus, D., Serra, E., Holl, M., Benjamin, K., Gordon, A., and Brent, R. (2008). Negative feedback that improves information transmission in yeast signalling. Nature *456*, 755-761.

Figure 1. ERK measurement in single Ras cell lines

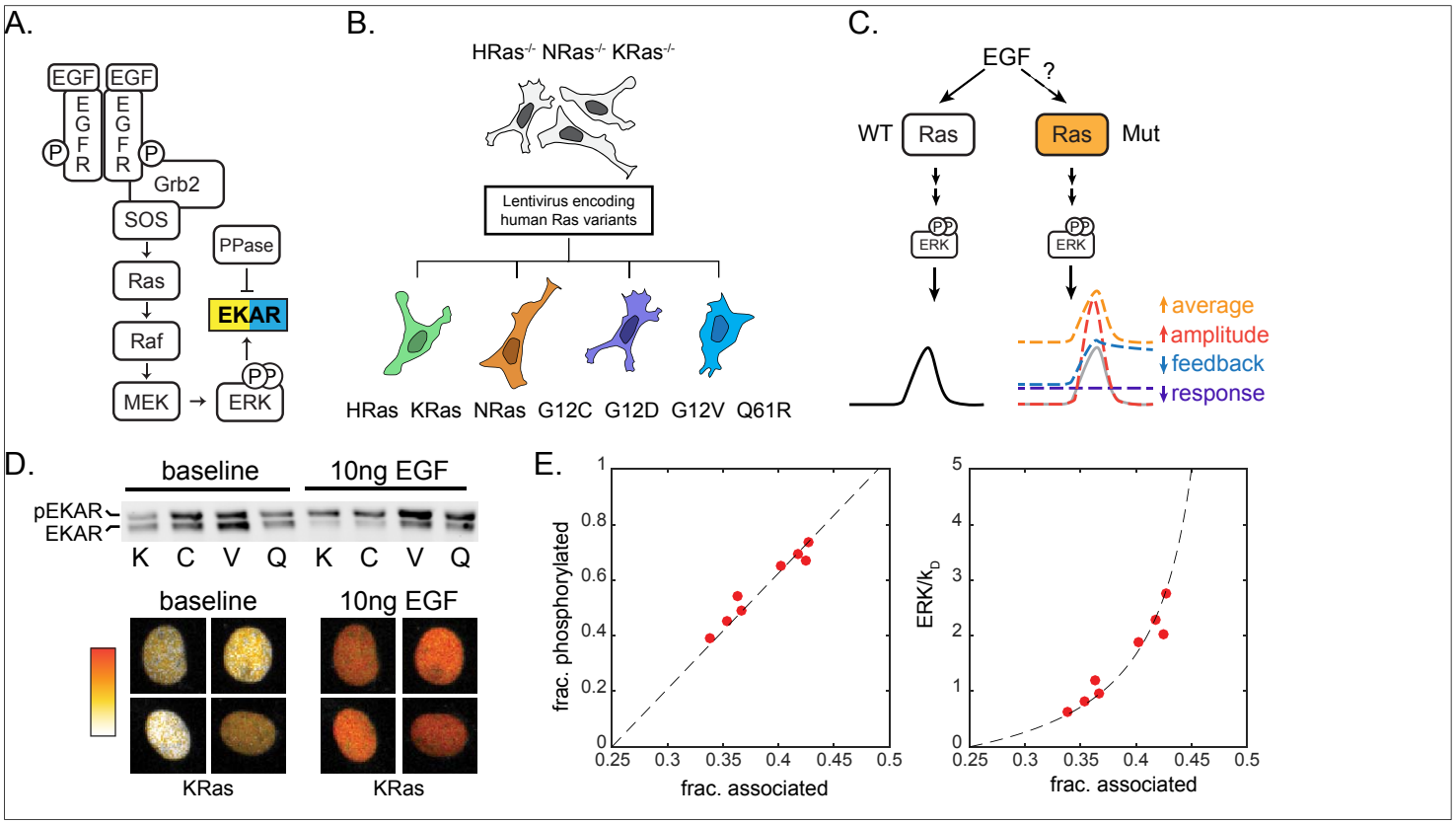

Figure 2. Single Ras isoform response profiles

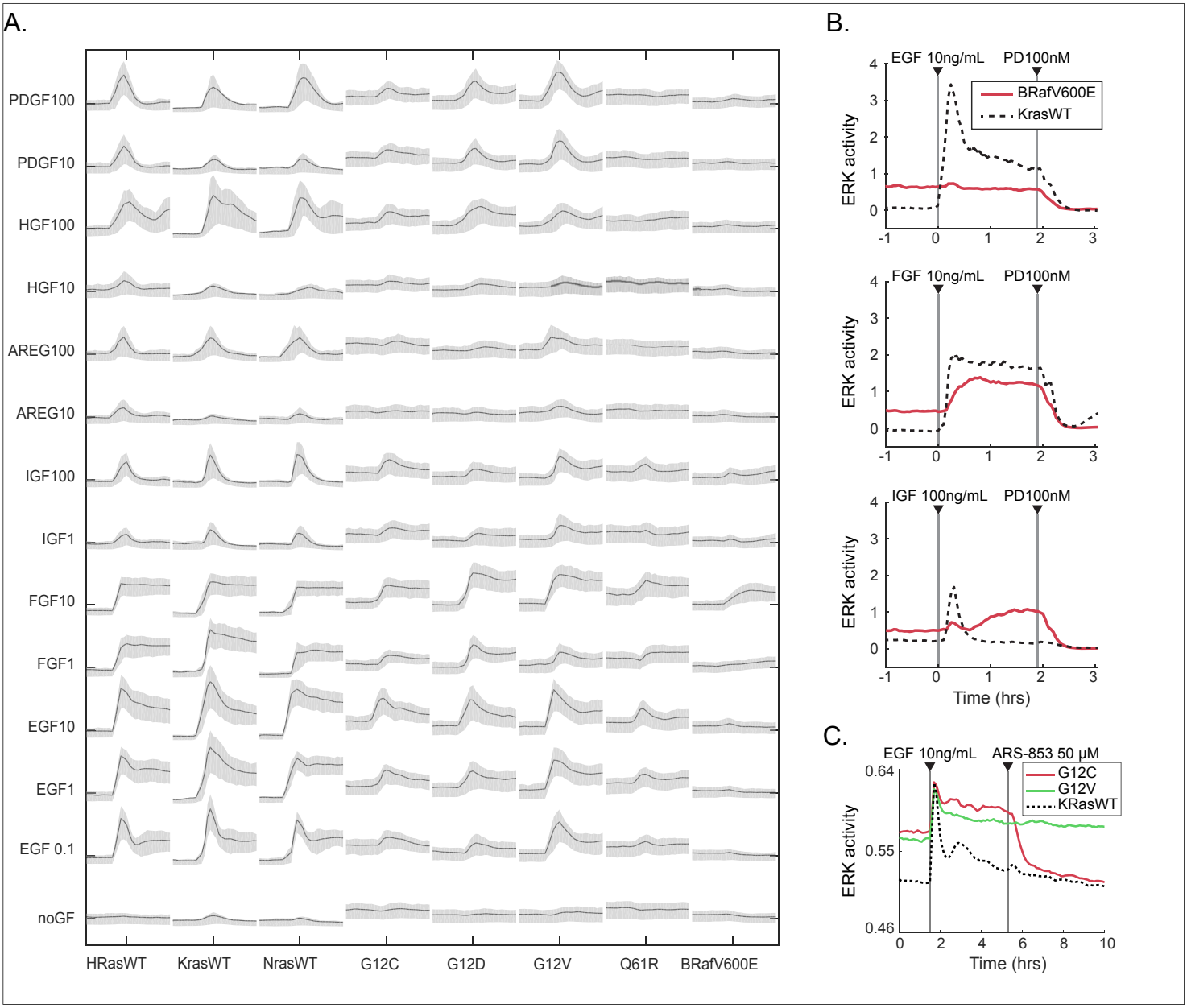

# Figure 3. ERK activity across Ras isoforms and mutants

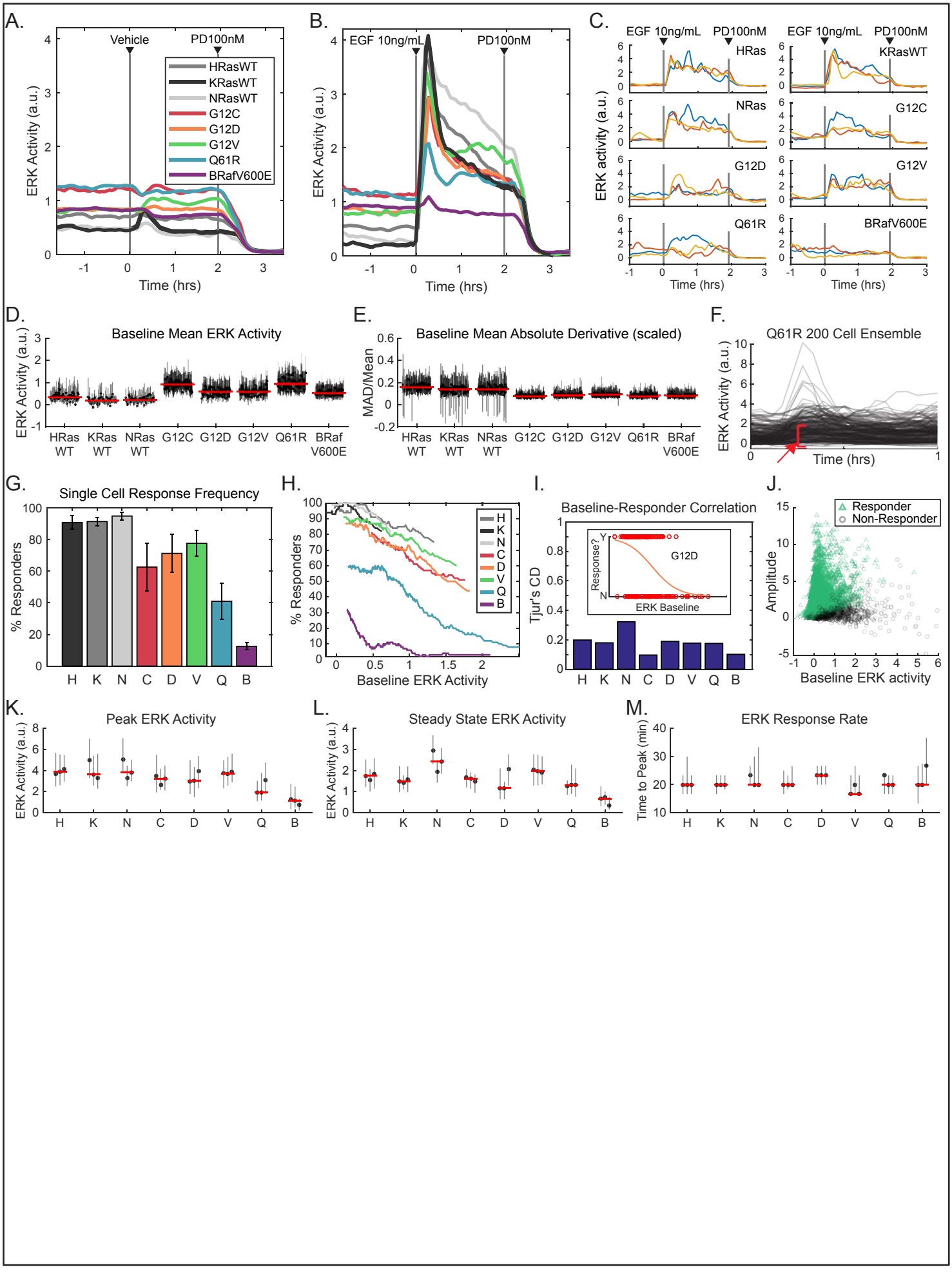

Figure 4. The range of ERK activity is maintained independently of pathway expression and Ras activity

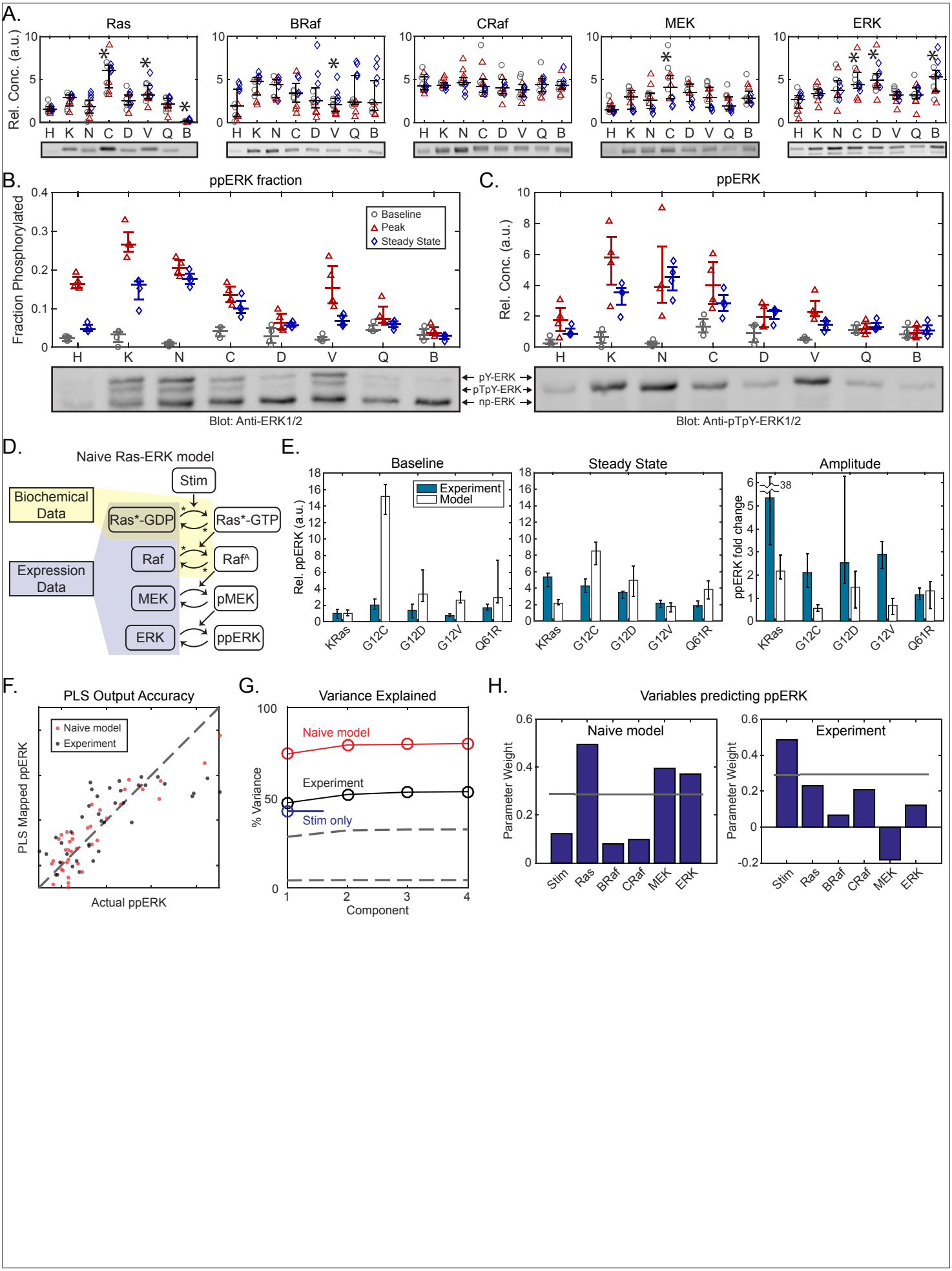

Figure 5. The function of ERK-mediated feedback in Ras mutants

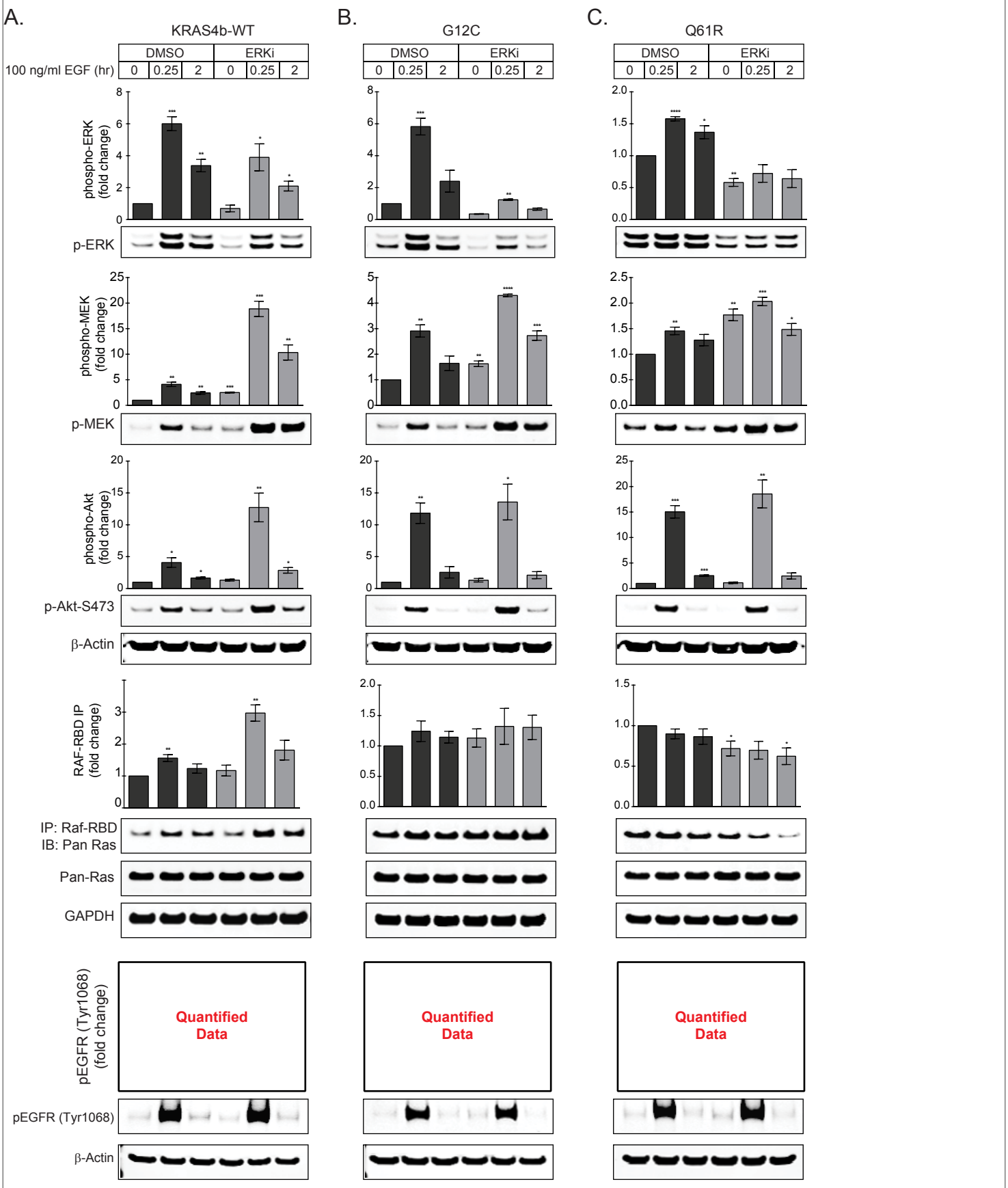

Figure 6. Phosphatases dynamically shape the function ERK output

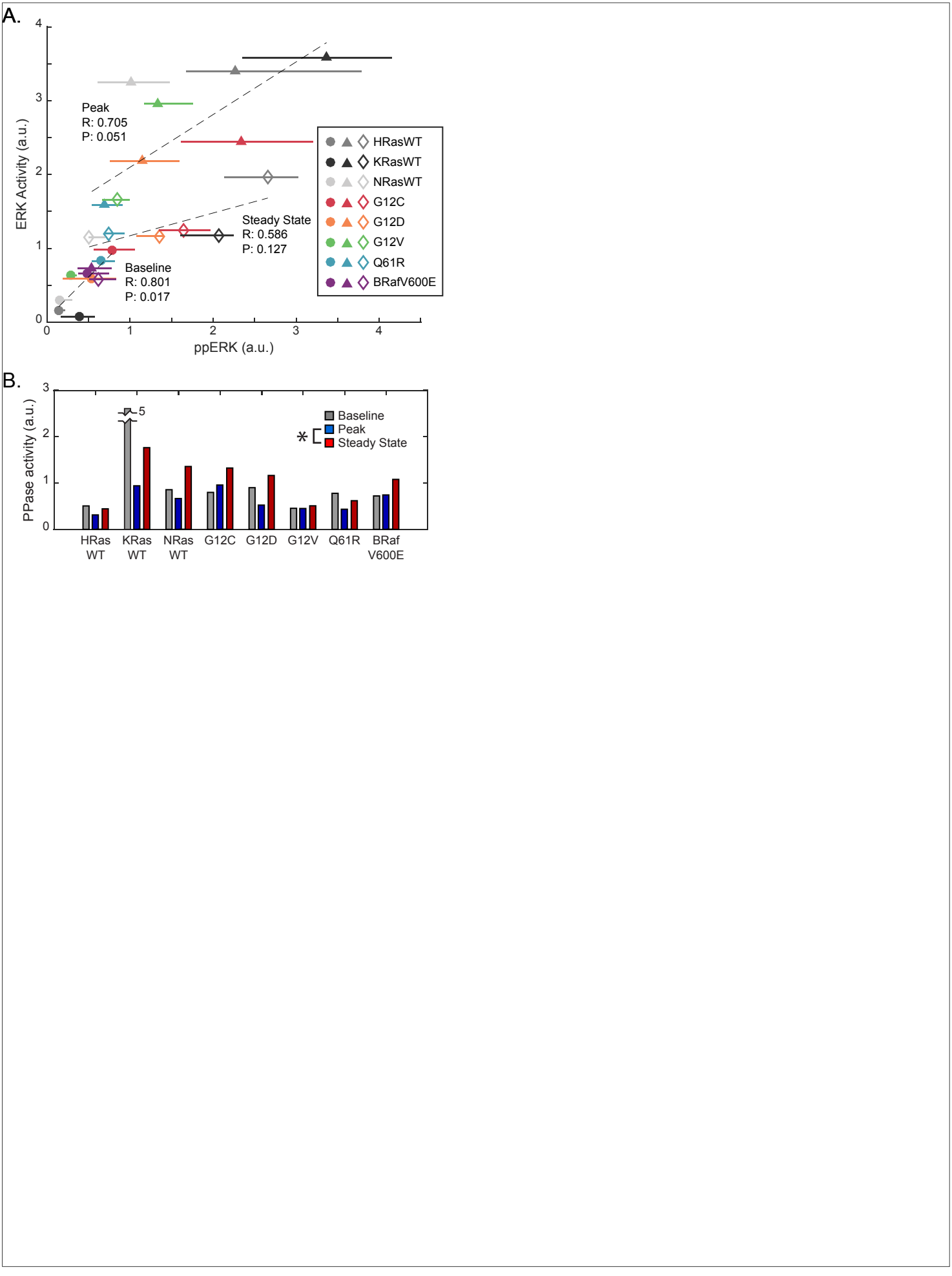

# Figure 7. Ras-ERK as a rescaling network

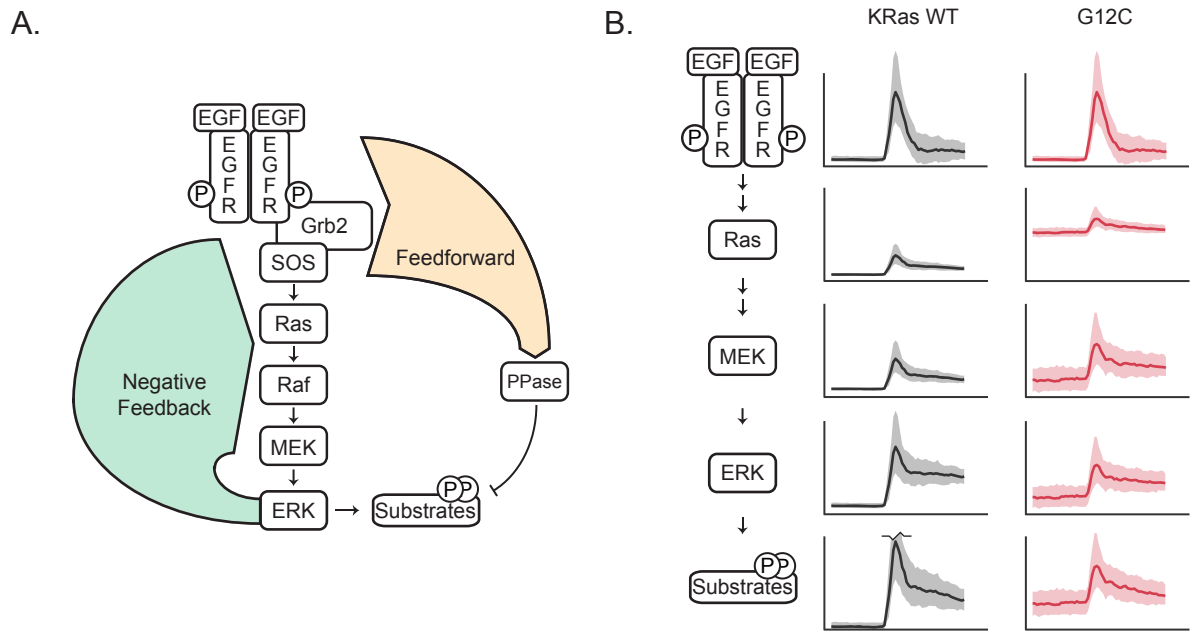


Legend:
Figure 7. The Ras-ERK pathway as a rescaling network. A) Schematic of functional, but distributed, regulatory effects evidenced in the pathway. B) Expected signaling at multiple nodes down the pathway, based on a combination of western blot and live-cell data from this study.